



doi:10.1016/j.gca.2004.01.012

Speciation of aqueous Ni(II)-carboxylate and Ni(II)-fulvic acid solutions: Combined ATR-FTIR and XAFS analysis

TIMOTHY J. STRATHMANN^{*,†} and SATISH C. B. MYNENI

Department of Geosciences, Princeton University, Guyot Hall, Princeton, NJ 08544, USA

(Received July 15, 2003; accepted in revised form January 14, 2004)

Abstract—Aqueous solutions containing Ni(II) and a series of structurally related carboxylic acids were analyzed using attenuated total reflection Fourier transform infrared spectroscopy (ATR-FTIR) and Ni *K*-edge X-ray absorption fine structure spectroscopy (XAFS). XAFS spectra were also collected for solutions containing Ni²⁺ and chelating ligands (ethylenediaminetetraacetic acid, nitrilotriacetic acid (NTA)) as well as soil fulvic acid. Limited spectral changes are observed for aqueous Ni(II) complexes with monocarboxylates (formate, acetate) and long-chain polycarboxylates (succinate, tricarballoylate), where individual donor groups are separated by multiple bridging methylene groups. These spectral changes indicate weak interactions between Ni(II) and carboxylates, and the trends are similar to some earlier reports for crystalline Ni(II)-acetate solids, for which X-ray crystallography studies have indicated monodentate Ni(II)-carboxylate coordination. Nonetheless, electrostatic or outer-sphere coordination cannot be ruled out for these complexes. However, spectral changes observed for short-chain dicarboxylates (oxalate, malonate) and carboxylates that contain an alcohol donor group adjacent to one of the carboxylate groups (lactate, malate, citrate) demonstrate inner-sphere metal coordination by multiple donor groups. XAFS spectral fits of Ni(II) solutions containing soil fulvic acid are consistent with inner-sphere Ni(II) coordination by one or more carboxylate groups, but spectra are noisy and outer-sphere modes of coordination cannot be ruled out. These molecular studies refine our understanding of the interactions between carboxylates and weakly complexing divalent transition metals, such as Ni(II). Copyright © 2004 Elsevier Ltd

1. INTRODUCTION

Metal–organic molecule interactions play a vital role in a number of chemical phenomena of interest, including mineral weathering, biologic acquisition of metals and their enzyme activity, environmental fate and toxicity, homogeneous and heterogeneous catalysis, materials synthesis, and contaminant treatment (Karlin, 1993; Gawel et al., 1996; Buerge and Hug, 1998; Ferry and Glaze, 1998; Hudson, 1998; Neys et al., 1998; Alcacio et al., 2001; Penn et al., 2001; Chen and Hsieh, 2002). Of different organic ligands that occur in the environment, carboxylates constitute the dominant fraction. These ligands occur in the environment as low-molecular-weight small chain organic molecules (e.g., acetate, malate) and as ill-defined polymeric macromolecules (e.g., humic substances) (Thurman, 1985). In addition, synthetic carboxylate-containing chelating agents are released into the environment from a variety of industrial and consumer activities. Interactions of both natural and synthetic carboxylates with soluble metals and mineral surfaces and their influence on the aforementioned environmental processes have been the subject of numerous investigations.

Most of the existing information on carboxylate–metal complexes is derived from thermochemical methods (Martell and Hancock, 1996; Blesa et al., 2000). Although this information is valuable in predicting the behavior of these complexes in the

natural systems, it does not provide unambiguous structural information that is necessary for the development of mechanistic models. Although researchers have begun complementing thermochemical information with spectroscopic measurements (Persson et al., 1998; Boily et al., 2000; Loring et al., 2001b), knowledge on metal–organic molecule interactions in aqueous solutions and at mineral–water interfaces is poor. In addition, a majority of spectroscopic studies have focused on strongly complexed metals, such as Hg(II) and Al(III) (Persson et al., 1998; Quilès et al., 1999); little is known about metals that exhibit weaker binding affinities. The goal of this investigation is to explore carboxylate interactions with a representative weakly complexing divalent metal ion, Ni(II). This study focuses on assessing the chemical variables and structural factors that control Ni(II)-carboxylate complex formation, evaluating the structures of these complexes, and assessing the relevance of Ni(II)-carboxylate complex formation with natural organic macromolecules (e.g., fulvic acid). This work represents part of a larger effort utilizing complementary in-situ spectroscopic techniques to characterize molecular interactions between metal ions and organic molecules, which will hopefully lead to a better understanding of interactions between organic macromolecules and soluble metals and mineral surfaces, and the influence of these interactions on various biogeochemical processes.

X-ray structure analysis of crystalline metal–carboxylates indicates that metals interact with carboxylates in four different ways (Fig. 1): i) outer-sphere (i.e., long-range electrostatic or H-bonding interactions of the carboxylate group with completely solvated metal), ii) inner-sphere monodentate (metal coordinated to one of the oxygen atoms of the carboxylate), iii) chelating bidentate (metal is coordinated by both oxygen atoms

* Author to whom correspondence should be addressed (strthmnn@uiuc.edu).

† Present address: University of Illinois, Environmental Engineering and Science Program, Department of Civil and Environmental Engineering, Newmark Civil Engineering Laboratory, 205 N. Mathews Avenue, Urbana, Illinois 61801.

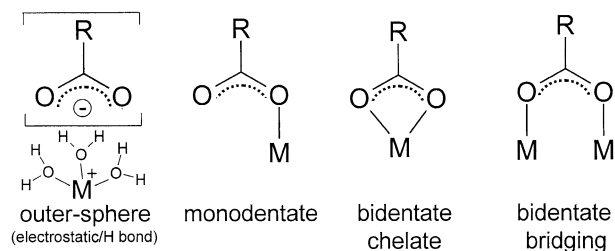


Fig. 1. General modes of metal-carboxylate coordination. Explicit water molecules are included in the outer-sphere structure to indicate that the metal ion retains its full hydration shell in this bonding mode; water molecules not shown on other structures for sake of simplicity. Adapted from Mehrotra and Bohra, 1983.

of the carboxylate), and iv) bridging bidentate (each oxygen atom of the carboxylate is coordinated to a separate metal ion) configurations (Deacon and Phillips, 1980; Mehrotra and Bohra, 1983). It is also established that metals can form multi-dentate complexes, wherein the metal is simultaneously coordinated by two or more suitably positioned donor groups in the same molecule (Bell, 1977; Dobson and McQuillan, 1999). However, the structures of metal-carboxylate complexes in noncrystalline systems, such as aqueous solution and solid/water interfaces, are more difficult to determine owing to a lack of long-range order and the addition of solvent interactions with both metal and ligand molecules.

In this investigation, a series of structurally related carboxylate ligands was studied to mimic the behavior of carboxylate groups in larger macromolecules (Fig. 2). Individual carboxylates studied include formate, acetate, lactate, oxalate, malonate, succinate, tricarballylate, malate, and citrate. These ligands vary in both the number of carboxylate donor groups and

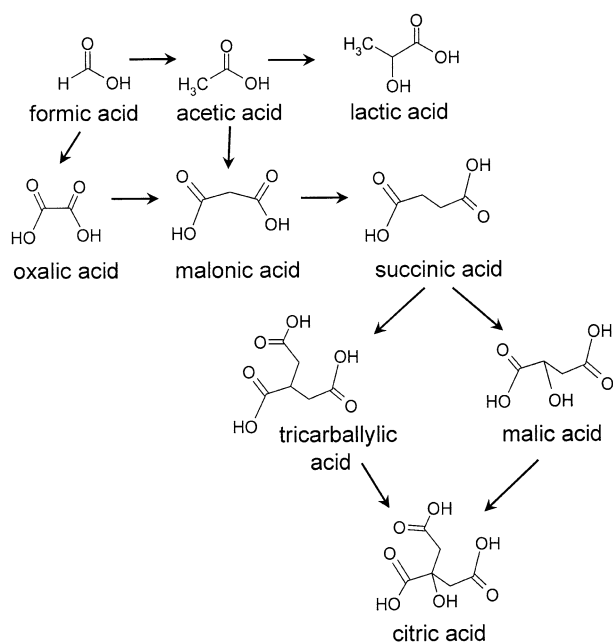


Fig. 2. Series of aliphatic carboxylic acids examined. Arrows indicate progression in structural complexity.

the number of atoms separating the carboxylates, and some of the selected ligands also contain an alcohol donor group adjacent to one of the carboxylates (α -OH substitution). In-situ infrared and X-ray spectroscopy were used to evaluate the chemical state of the ligand and the metal coordination environment, respectively. These spectroscopy methods are well suited for probing the structure and binding in metal-carboxylate complexes in aqueous solutions and at interfaces. Carboxylate groups have characteristic infrared-active vibrational bands that are sensitive to changes in proton and metal coordination (Mehrotra and Bohra, 1983; Cabaniss and McVey, 1995; Quilès et al., 1999), while X-ray spectra of metals and their organic complexes can provide information on the metal coordination environment (Koningsberger and Prins, 1988). Molecular spectra for each ligand at different pH and metal-to-ligand concentration ratios ($[M]/[L]$) were compared with the Ni(II)-carboxylate speciation predicted using previously reported thermodynamic formation constants (Martell et al., 1997). Although the speciation calculations contain inherent errors due to ionic strength effects, they provide a rough estimate of the species that are thought to predominate under different solution conditions. X-ray spectra were also collected for solutions containing Ni(II) and soil fulvic acid, and these results were compared to those obtained for the low-molecular-weight carboxylates.

2. EXPERIMENTAL

2.1. Sample Preparation

Reagent grade $\text{NiCl}_2 \cdot 6\text{H}_2\text{O}$, $\text{Ni}(\text{NO}_3)_2 \cdot 6\text{H}_2\text{O}$, $\text{Ni}(\text{ClO}_4)_2 \cdot 6\text{H}_2\text{O}$, NaCl, NaOH, HCl, D_2O , DCl, NaOD, sodium formate, sodium acetate, sodium DL-lactate, disodium oxalate, malonic acid, succinic acid, tricarballylic acid, DL-malic acid, L-sodium malate, trisodium citrate, disodium ethylenediaminetetraacetate, and sodium nitrilotriacetate from Sigma-Aldrich or Fisher were used in this investigation. Fulvic acid used in this investigation was standard Elliott soil fulvic acid (2S102F), obtained from the International Humic Substance Society. Aqueous solutions of the above salts were prepared using deionized water, and pH was adjusted using HCl and NaOH (DCl and NaOD for D_2O samples). Samples were reacted for at least 12 h before spectroscopic analysis to ensure equilibrium was achieved in solutions. This is relevant because Ni(II)-water exchange rates are on the order of 10^4 s^{-1} (Huheey et al., 1993). Solution pH was measured during sample preparation and after reaction using an Orion Model 525A pH meter outfitted with an Orion semimicro combined probe. All glassware used in this study was washed with 1M HNO_3 and rinsed with deionized water before use.

Metal, ligand, and electrolyte concentrations used in this investigation are higher than those found in natural waters, but concentrations this high could occur at contaminated sites. High concentrations were used because: i) detailed molecular spectroscopy studies cannot be conducted at concentrations found in natural waters, ii) low stability constants for the formation of selected Ni(II)-carboxylate complexes required the use of high nickel-to-ligand and ligand-to-nickel ratios, and iii) high electrolyte concentrations were required to ensure that spectral changes were not the result of ionic strength changes. Except for oxalate, all other Ni(II)-carboxylate solutions are soluble at concentrations examined in this study. Rapid precipitation of Ni(II)-oxalate complexes at oxalate concentration $>10 \text{ mM}$ prevented the examination of soluble complexes using both X-ray and attenuated total reflection Fourier transform infrared spectroscopy (ATR-FTIR) methods (details of methods discussed later). For infrared spectroscopy studies, spectra were obtained for a precipitate that forms slowly in dilute (2.5 mM) equimolar Ni(II)-oxalate solutions. The spectral intensity was low immediately after mixing of the stock solutions, but increased dramatically over a 20-h time period as a visible precipitate film formed on the surface of the horizontal internal reflection crystal used in this study.

The formation of the surface film effectively concentrated Ni(II)-oxalate within the penetration path length of the ZnSe ATR crystal (1–2 μm). Because dilute oxalate solutions were used, spectral contributions from dissolved oxalate species in the overlying aqueous phase are negligible compared to the intensity of the contributions from the precipitate. High concentration of NaCl background electrolyte was used for a majority of solutions to ensure constant ionic strength during spectroscopic titrations; this practice ensures that observed spectral changes are due to metal coordination and not simply to changes in solution ionic strength. Previous studies have also utilized high salt concentrations to reduce nontarget spectral artifacts and to isolate spectral features of the complexes of interest (Loring et al., 2001a; Loring et al., 2001b).

2.2. Thermodynamic Speciation of Ni(II)-Carboxylates

Equilibrium speciation calculations were performed for Ni(II)-carboxylate solutions using the software HYDRAQL (Papelis et al., 1988) and previously reported equilibrium stability constants (Martell et al., 1997). All calculations were conducted using conditional stability constants that have been previously measured at ionic strength conditions corresponding to those used for infrared and X-ray analysis (0.05–2 mol/L). Conditional stability constants for a given Ni(II)-carboxylate species can vary considerably over the range of ionic strength conditions examined here, in some cases by a log unit or more (Martell et al., 1997). When stability constants were not available at the ionic strengths in question, they were estimated using activity coefficients that were calculated using the Davies equation (Davies, 1962). Although the Davies equation can adequately account for changes in conditional stability constants that occur over limited changes in ionic strength, this empirical relationship is strictly valid for ionic strength <0.5 mol/L (Stumm and Morgan, 1996). It follows that using this relationship to estimate unavailable conditional stability constants for high ionic strength conditions (e.g., 2 mol/L) can lead to considerable errors in the final predicted Ni(II)-carboxylate speciation. In addition, stability constant measurements were typically made at much lower total ligand and metal concentrations than those examined here, particularly for samples prepared for infrared spectroscopy. Therefore, results of equilibrium calculations presented here should only be considered rough estimates of speciation. This statement is especially true for some of the solutions containing high metal-to-ligand ratios.

2.3. ATR-FTIR Spectroscopy

ATR-FTIR spectra were collected using a Bruker IFS 66v/S spectrometer equipped with a SpectraTech horizontal ATR accessory, a mid IR source, a KBr beam splitter, and a liquid N₂-cooled Mercury Cadmium Telluride (MCT) detector. The ATR accessory consists of trough-style 45° ZnSe or AMTIR crystal (12 internal reflections). Infrared spectra were acquired at 2 cm⁻¹ resolution and resulted from an average of at least 2000 scans. Slit openings in the instrument were set to 4 or 6 mm. The spectrum of deionized water (or D₂O in the case of deuterated samples) was used as background for all samples. In addition, strong spectral contributions from metal-solvated water were subtracted using the spectra of carboxylate-free solutions containing the same concentration of Na⁺ and Ni²⁺ (from chloride salts). Spectra for solutions of equivalent H⁺ concentration were also subtracted for samples pH ≤ 3 . Although care was taken during the subtraction procedure, spectral contributions from $\delta(\text{H-O-H})$ (~1630 cm⁻¹), $\delta(\text{H-O-D})$ (~1460 cm⁻¹), and $\delta(\text{D-O-D})$ (~1200 cm⁻¹) cannot be completely eliminated, and care should be taken when interpreting spectral features at these energies. Spectral subtractions and analysis were conducted using the software package Grams/AI (Thermo Galactic).

2.4. XAFS Spectroscopy

X-ray absorption fine structure (XAFS) spectra were collected for the Ni-absorption edge at the Stanford Synchrotron Radiation Laboratory (SSRL) on beamlines 2-3 and 4-3 using a Si(111) or Si(220) double crystal monochromator. Incident beam was detuned by 50% above the Ni-absorption edge to reject higher-order harmonics. Slits were kept narrow (1 \times 10 mm) for collecting X-ray absorption near edge structure (XANES) spectra when compared to those used for

extended X-ray absorption fine structure (EXAFS) spectra collection (2 \times 10 mm). Aqueous solutions were placed in 5-mm-thick slotted acrylic plates and contained using X-ray clean Kapton tape for spectral collection. The Kapton tape was pretreated with 6N NaOH to remove soluble organic films. Samples were kept at 45° to the incident beam, and the fluorescence spectra were collected at room temperature using a 13-element Ge detector (dilute samples) or a Lytle detector filled with Ar (for concentrated samples). At least three scans were collected for XANES spectral analysis, and at least 10 scans were collected for EXAFS spectral analysis. The spectra were averaged and energy calibrated (against a Ni(0) foil with the inflection point of absorption edge set to 8331.6 eV) before analysis.

XAFS spectral analysis was accomplished using EXAFSPAK, SixPACK, and IFEFFIT (George and Pickering, 1995; Newville, 2001; Webb, 2003). The background in the XAFS spectra was subtracted using either a first or second order polynomial (gaussian function; for dilute samples). Typically a first or second order spline is used for the above-edge normalization for the XANES analysis, and third order spline is used to extract the XAFS. Normalized $\chi(k)$ functions and Fourier transforms were extracted using SixPACK. The XAFS spectra were converted from energy to k space by setting E_0 at 8345 eV. The AUTOBK algorithm was used for background removal (Rbkg = 0.7; spline fitting region = 1.145–16.2 k ; low clamp = none; high clamp = strong; k weight = 3; Kaiser-Bessel window sill width = 1) (Newville et al., 1993). The resulting $\chi(k)$ functions were weighted by k^3 to compensate for damping of the EXAFS amplitude with increasing k . Appropriate regions of the $\chi(k)$ functions were then Fourier transformed to obtain radial structure functions (RSFs). A Kaiser-Bessel window with a smoothing parameter of 3 \AA^{-1} was used to suppress artifacts resulting from the finite Fourier filtering ranges used. The software packages ATOMS and FEFF8 were used to generate ab initio phase and amplitude functions for single and multiple scattering paths in nickel acetate tetrahydrate (Ankudinov et al., 1998; Nicolai et al., 1998; Ravel, 2002). Results were similar when phase and amplitude functions were obtained from crystalline nickel citrate (Baker et al., 1983).

Structural parameters for aqueous Ni(II) complexes were obtained by the following spectral fitting procedure. First, single shell fits of the intense peak in RSF were carried out in R space between 0.9 and 2.1 \AA using a single FEFF-generated Ni-O single scattering path. The coordination number (CN), average Ni-O bond distance (R), Debye-Waller factor (σ^2), and phase shift (ΔE_0) were used as adjustable fitting parameters. The amplitude reduction factor (S_0^2) was fixed at 0.86 for all fits. The structural parameters obtained by fitting the Fourier-filtered $\chi(q)$ functions were similar to values obtained by fitting in R space. Selected Ni(II)-organic complexes contained an additional backscatter peak between 2.0–2.8 \AA in the RSF, which was attributed to the second-shell carbon atoms present in the Ni(II)-carboxylate complexes. Two-shell fitting was carried out in R space over the range of the first two shells (0.9–2.8 \AA), and structural parameters for each shell were optimized. ΔE_0 values were fixed at those determined from single shell fits, thereby eliminating one adjustable parameter (O'Day et al., 1994). The first-shell structural parameters determined from single and two-shell fits were similar. In addition, optimized second-shell structural parameters were similar when first-shell parameters were either fixed or floated during the fitting procedure.

3. RESULTS

3.1. ATR-FTIR Spectroscopy

Infrared spectroscopy is sensitive to variations in the carboxylate moiety, but not to Ni(II)-centered vibrational modes in aqueous solutions (e.g., Ni-O stretches; Pike et al., 1993). The carboxylate group changes its chemical state upon protonation or metal complexation, and its vibrational spectra can provide information on the nature of metal-carboxylate interactions (Mehrotra and Bohra, 1983; Cabaniss and McVey, 1995; Quilès et al., 1999). Relevant spectral information includes the changes in the energy, shape, and width of vibrational bands. Metal complexation of the carboxylate group typically involves

Table 1. Infrared peak positions for protonated, ionized, and Ni(II)-complexed carboxylate species.

Ligand	Fully protonated species			Deprotonated (uncomplexed) and Ni(II)-complexed species					
	$\nu(\text{C}=\text{O})$	$\nu(\text{C}-\text{OH})$	$\nu_{\alpha}(\text{C}-\text{OH})^c$	[M]/[L]	pH	% complexed ^d	$\nu_{\text{as}}(\text{CO}_2)^e$	$\nu_{\text{s}}(\text{CO}_2)^e$	$\nu_{\alpha}(\text{C}-\text{OH})^c$
Formate ($\text{p}K_{\text{a}} = 3.5$) ^a	1720	1212		0	6.5	0	1581	1351	
				5	5.0	18	1581	1353	
				50	5.0	44	1582	1355	
Acetate ($\text{p}K_{\text{a}} = 4.6$) ^a	1714	1279		0	6.8	0	1552	1415	
				5	6.0	26	1550	1418	
				50	6.0	54	1548	1423	
Lactate ($\text{p}K_{\text{a}} = 3.6$) ^a	1725	1230–1460 (1238) ^b	1132	0	9.9	0	1575	1417	1129
				4	5.5	72	1590	n/a ^h	1119
				40	5.5	90	1592	n/a ^h	1119
Oxalate ($\text{p}K_{\text{a}} = 1.0, 3.7$) ^a	1740	1228		0	6.6	0	1570	1308	
				1	6.0	>99	1620 ^{f,g}	1360 ^{f,i} , 1317 ^{f,j}	
Malonate ($\text{p}K_{\text{a}} = 2.6, 5.1$) ^a	1722	1170–1430 (1217) ^b		0	8.0	0	1563	1357	
				1	6.0	89	1590, 1570*	1362	
				4	6.0	>99	1589*, 1568(s)	1365	
Succinate ($\text{p}K_{\text{a}} = 4.0, 5.1$) ^a	1719	1180–1420 (1238) ^b		50	6.0	>99	1590*, 1568(s)	1373	
				0	9.3	0	1553	1397, 1420(ws)	
				5	6.0	36	1552	1420, 1401*	
Malate ($\text{p}K_{\text{a}} = 3.2, 4.5$) ^a	1725	1190–1440 (1231) ^b	1109	50	6.0	84	1550	1421*, 1402	
				0	9.5	0	1568	1395	1096
				1	6.0	71	1600, 1567*	1426*, 1399	1081
Tricarballylate ($\text{p}K_{\text{a}} = 3.4, 4.4, 5.5$) ^a	1720	1180–1430 (1232) ^b		20	6.0	>99	1600, 1567*	1427*, 1399	1082
				0	9.6	0	1559	1394	
				1	6.0	62	1558	1395	
Citrate ($\text{p}K_{\text{a}} = 2.9, 4.4, 5.6$) ^a	1724	1210–1440 (1228) ^b	1135	5	6.0	96	1557	1395	
				50	6.0	>99	1554	1402	
				0	8.0	0	1569	1391	1093
				1	7.0	98	1602, 1570*	1420*, 1393	1070
				10	6.0	>99	1599, 1568*	1420*, 1394	1072

^a $\text{p}K_{\text{a}}$ values from the database Critical (Martell et al., 1997). All $\text{p}K_{\text{a}}$ values are conditional equilibrium constants valid for 1 M ionic strength, except oxalate, malonate (0.5 M), and citrate (0.1 M).

^b Unable to resolve an individual $\nu(\text{C}-\text{OH})$ peak position because spectra contain multiple overlapping peaks in this region. Number in parenthesis indicates most prominent pH-dependent peak within the range.

^c Refers to the $\nu(\text{C}-\text{OH})$ band for the alcohol group located on the carbon atom adjacent to one of the carboxylate groups.

^d Represents the predicted fraction of the ligand that is complexed by Ni(II) using previously reported equilibrium formation constants (Martell et al., 1997).

^e Asterisk represents the position of the larger peak component. (s) = shoulder. (ws) = weak shoulder.

^f Spectrum for precipitate that forms in solution containing 2.5 mM Ni(II) + 2.5 mM oxalate.

^g Absorption band centered at 1620 cm^{-1} is attributed to $\nu_{\text{as}} + \delta(\text{H}-\text{O}-\text{H})$.

^h Unable to assign frequency; absorption too weak and overlaps with other vibrational modes.

ⁱ Attributed to ν_{s} coupled with $\nu(\text{C}-\text{C})$.

^j Attributed to ν_{s} coupled with $\delta(\text{O}-\text{C}-\text{O})$.

deprotonation of the latter. To evaluate metal–carboxylate interactions, it is important to evaluate how vibrational spectra of carboxylates change upon deprotonation in aqueous solutions. This study focuses on the variations in the carboxylate vibrations as a function of: i) pH in Ni(II)-free solutions, ii) [M]/[L] ratio at a fixed pH, and iii) pH in solutions containing a fixed [M]/[L]. Speciation calculations were used to estimate the optimum range of [M]/[L] and pH to examine for each ligand. Relatively high [M]/[L] were used for some weakly complexing carboxylates (i.e., those with low Ni(II)-ligand complex stability constants) in an effort to maximize the extent of ligand complexation by Ni(II). Higher pH was used to ensure complete deprotonation of all carboxylate groups in (ii), but low enough to prevent precipitation of $\text{Ni}(\text{OH})_2(\text{s})$.

3.1.1. Protonation/deprotonation of carboxylates

The $\text{p}K_{\text{a}}$ values of mono and poly carboxylates examined in this study range from 1.0 to 5.6 (Table 1; Martell et al., 1997).

Infrared spectra collected for different protonation states (e.g., L^{n-} , HL^{1-n} , H_2L^{2-n}) of carboxylates agree with those reported earlier (Cabaniss and McVey, 1995; Cabaniss et al., 1998), and the spectral variation for most of the ligands is also consistent with the reported $\text{p}K_{\text{a}}$ values (Fig. 3; Table 1). For oxalic, malonic, and citric acid, expected spectral changes for their first deprotonation occurs at pH values higher than those predicted by the reported $\text{p}K_{\text{a}1}$ values. This discrepancy may have been caused by errors in pH measurements under highly acidic conditions (pH probe was calibrated using pH 4, 7, and 10 buffers). However, the experiments evaluating Ni(II) complexation by these carboxylates were conducted within the calibrated pH range.

In the protonated state, carboxylic acids exhibit a distinct band between $1714\text{--}1740\text{ cm}^{-1}$ corresponding to the carbonyl stretching ($\nu(\text{C}=\text{O})$), and a weak band between $1150\text{--}1450\text{ cm}^{-1}$ corresponding to the symmetric and asymmetric stretching of the C-OH ($\nu(\text{C}-\text{OH})$). Although the high-energy band

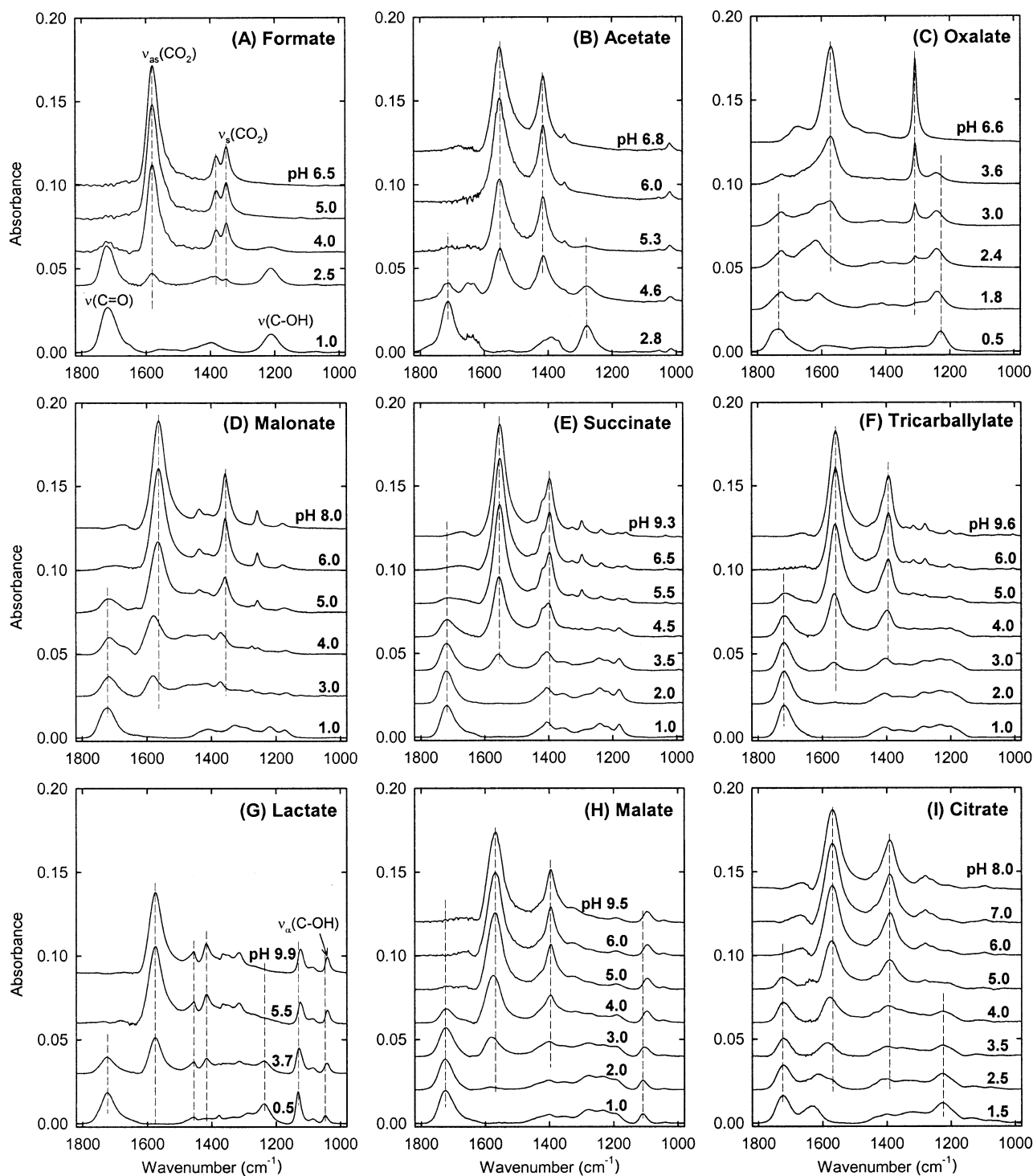


Fig. 3. FTIR spectra of carboxylate ligands as function of pH (Ni-free solutions). Solution conditions: (A) 50 mM formate, (B) 50 mM acetate, (C) 50 mM oxalate, (D) 50 malonate, (E) 50 mM succinate, (F) 50 mM tricarballylate, (G) 100 mM lactate, (H) 50 mM malate, and (I) 25 mM citrate. All solutions contain 1 mol/L NaCl, except oxalate (0.5 mol/L), malonate (0.4 mol/L), and citrate (0.125 mol/L). Spectral intensities normalized to 50 mM carboxyl group concentration.

can be identified unambiguously, identification of the low-energy band is complicated by the presence of several peaks in this region. These low-energy bands originate from variations in the intramolecular and intermolecular interactions between

carboxylic groups and other moieties (e.g., hydroxyls, amines), vibrational coupling between different modes (e.g., C-O, C-C, C-H), and from the bending vibrations of CH₂ and CH₃ groups (Schmelz et al., 1959). Often, the most intense pH-dependent

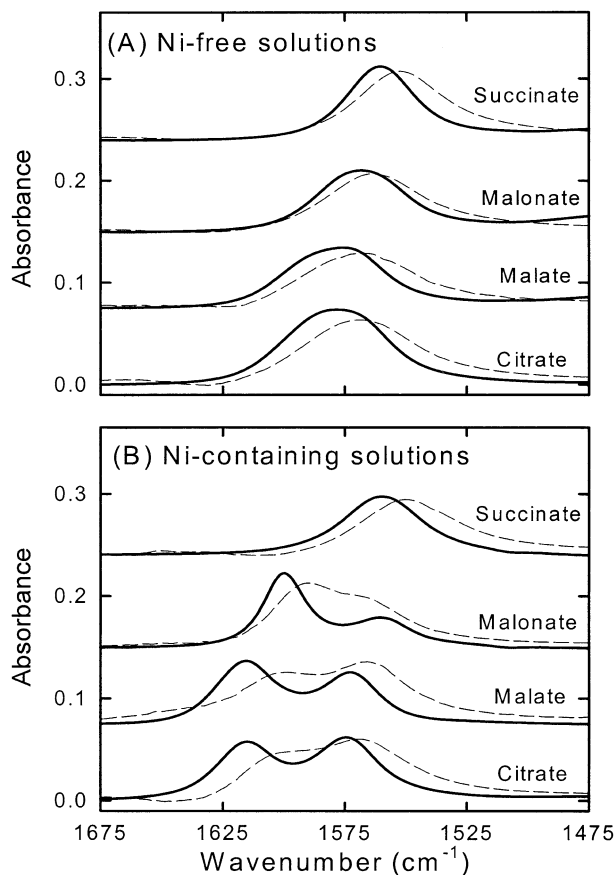


Fig. 4. Close-up of the asymmetric CO_2 stretching region of the IR spectra of (A) Ni(II)-free and (B) Ni(II)-complexed carboxylates in H_2O (dashed lines) and D_2O (solid lines). Solution conditions: pH or pD 6.0, 20 mM carboxylate, 40 mM Ni(II) (malate, citrate) or 1000 mM Ni(II) (succinate, malonate).

band located between $1150\text{--}1400\text{ cm}^{-1}$ is considered to be caused by the $\nu(\text{C-OH})$ (Cabaniss et al., 1998). As pH increases, the carboxylic acid groups deprotonate and the vibrational bands discussed above shift to different energies. All carboxylates examined in this study are fully deprotonated at neutral pH, and these molecules exhibit two prominent peaks, one between $1550\text{--}1581\text{ cm}^{-1}$, and another between $1308\text{--}1417\text{ cm}^{-1}$. These bands correspond to the asymmetric ($\nu_{\text{as}}(\text{CO}_2)$) and symmetric ($\nu_{\text{s}}(\text{CO}_2)$) stretching vibrations of the deprotonated COO^- , respectively (hereafter referred to as ν_{as} and ν_{s} , respectively). For the reasons discussed above, the ν_{s} contribution is spread over several small bands between $1300\text{--}1500\text{ cm}^{-1}$ region for some molecules (e.g., formate, succinate, lactate). Replacement of H_2O with D_2O alters the ν_{as} band of all carboxylates without any influence on the ν_{s} band. For each carboxylate examined, ν_{as} in D_2O is shifted to slightly higher frequencies ($<10\text{ cm}^{-1}$) when compared to the equivalent H_2O solutions (Fig. 4A).

In addition to the above bands, a weak absorption band ($\nu_{\alpha}(\text{C-OH})$) between $1090\text{--}1130\text{ cm}^{-1}$ is also observed for lactate, malate, and citrate, which may correspond to the C-O stretching of an alcohol group that is adjacent to one of the carboxylate groups in the structure of these ligands ($\alpha\text{-OH}$;

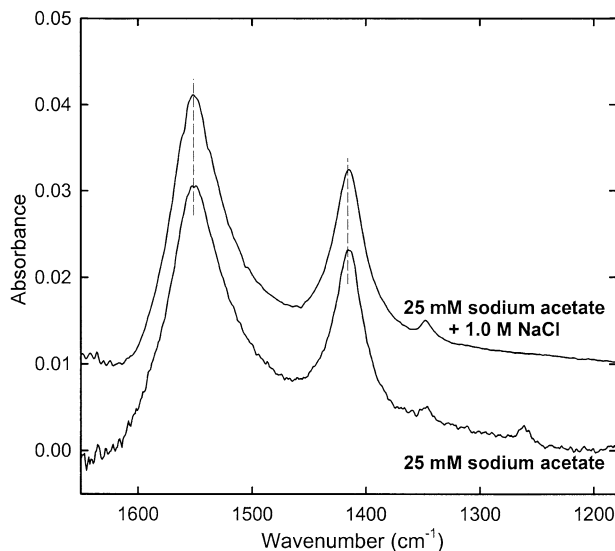


Fig. 5. Effect of Na^+ concentration on the FTIR spectra of acetate. Solution conditions: pH 6.0, 25 mM sodium acetate, either 0 or 1 mol/L NaCl.

Cabaniss et al., 1998). The alcohol group does not deprotonate in the pH range examined. However, $\nu_{\alpha}(\text{C-OH})$ shifts to lower frequencies upon deprotonation of the neighboring carboxylate groups. When H_2O is replaced by D_2O for malate and citrate, the frequency of this band is unaffected, but the $\nu_{\alpha}(\text{C-OH})$ peak is broader in D_2O than in H_2O . The lack of change in the frequency suggests that the alcoholic proton is not exchanged with deuterium ions from the solvent. Spectral broadening results from hydrogen bonding between the alcohol group and the solvent D_2O molecules.

3.1.2. Nickel complexation with carboxylates

3.1.2.1. Sodium complexation with carboxylic acids. It is necessary to evaluate how the background electrolyte (Na^+ , Cl^-) interacts with the carboxylates before the effects of Ni(II) complexation can be properly evaluated. Speciation calculations predict that a significant fraction of the carboxylates should be complexed by Na^+ (e.g., $\sim 26\%$ of 25 mM acetate is complexed in 1 mol/L Na^+ solution). However, our measurements indicate that infrared spectra of carboxylates are insensitive to a large variation in dissolved NaCl concentration. For example, 25 mM sodium acetate solution is unaffected by the addition of 1 mol/L NaCl to solution, despite the fact that 26% of the free acetate is predicted to be complexed to Na^+ in these solutions (Fig. 5). Hind and coworkers reported similar results ($<1\text{ cm}^{-1}$ shift for ν_{s} and ν_{as} for a $[\text{M}]/[\text{L}]$ of 40) for oxalate solutions containing a variety of alkali metal ions (Hind et al., 1998). These results indicate that either Na^+ complexation does not modify the spectral properties of the carboxylate group or that previously measured stability constants are overpredicting the degree of Na^+ complexation. The former scenario is consistent with the presumed dominance of outer-sphere Na-carboxylate interactions (Fig. 1). When compared to the effects of Na^+ addition, Ni^{2+} addition has a pronounced effect on the spectra of most of the carboxylates examined.

3.1.2.2. Nickel complexation with monocarboxylic acids.

Among the examined monocarboxylates, speciation calculations indicate that several of them form complexes with Ni(II) in aqueous solutions. Reported stability constants for Ni(II) coordination by the monocarboxylate ligands examined are relatively small (Martell et al., 1997). Consequently, Ni(II) was added to solution in considerable stoichiometric excess to affect the complexation of a significant fraction of the ligands present. For example, only 44% of formate and 54% of acetate are predicted to be complexed to Ni(II) at pH 6 when $[M]/[L] = 50$ (Table 1). The ν_{as} and ν_s bands shifted by $+1\text{ cm}^{-1}$ and $+4\text{ cm}^{-1}$ for formate, and -4 cm^{-1} and $+8\text{ cm}^{-1}$ for acetate, respectively, when compared to those of uncomplexed ligands (Fig. 6A-B). In addition, the ν_s broadens significantly for acetate (full width at half maximum, FWHM, increases by 40%), probably due to overlapping spectral contributions from uncomplexed and Ni(II)-complexed acetate species present in solution. The observed spectral changes are smaller in magnitude when compared to those observed in acetate solutions containing the strongly complexing Al(III) and Hg(II) ions (Persson et al., 1998; Quilès et al., 1999).

3.1.2.3. Nickel complexation with polycarboxylic acids. Several ligands that contain multiple carboxylate donor groups exhibit larger stability constants for metal-carboxylate complex formation, and this has been attributed to their ability to form multidentate complexes (Bell, 1977). In this study, Ni(II) complexation of dicarboxylates, oxalate, malonate, and succinate are evaluated. Speciation calculations predict nearly 100% of oxalate, a C_2 dicarboxylate, is complexed by Ni(II) in equimolar solutions at neutral pH. The resulting complex(es) precipitates rapidly even in dilute solutions, and infrared spectra could not be obtained for soluble species (details in “Experimental” section). Spectra collected for this precipitate have features that are similar to that of aqueous Al(III)-oxalate complex (Fig. 6C) (Axe and Persson, 2001).

Malonate, a C_3 dicarboxylate ligand, also strongly complexes with Ni(II) at relatively low $[M]/[L]$; 89% is predicted to be complexed at pH 6.0 when $[M]/[L] = 1$ (Fig. 6D). The ν_{as} peak in uncomplexed malonate appears to broaden slightly (FWHM increases by 10%) and split into two components upon Ni(II) addition. The frequency of one component remains relatively unchanged, whereas a second component shifts by $+25\text{ cm}^{-1}$ relative to ν_{as} of Ni(II)-free solutions. The relative contribution of the higher frequency component increases with increasing $[M]/[L]$. The ν_s peak also broadens considerably (FWHM increases by 66%) and shifts to higher frequency by 15 cm^{-1} when Ni(II) is added. A peak at 1440 cm^{-1} , assigned to the $\delta(\text{CH}_2)$, increases in intensity as Ni(II) is added to solution. Dobson and McQuillan (1999) attributed a similar trend in the infrared spectra of malonate adsorbed on metal oxide surfaces (TiO_2 , Al_2O_3 , Ta_2O_5 , and ZrO_2) to increased strain in the bridging methylene group resulting from bidentate metal complexation by both carboxylate groups.

As the distance between carboxylate groups increases, such as in succinate (a C_4 dicarboxylate), predicted Ni(II) complexation drops considerably, presumably due to the decreased stability of the larger chelate ring sizes (Bell, 1977; Martell et al., 1997). For example, at pH 6.0 and $[M]/[L] = 50$, speciation calculations suggest only 84% of succinate is complexed by Ni(II). This is reflected by the infrared spectra of succinate,

which shows that the ν_{as} shifts by -3 cm^{-1} as $[M]/[L]$ increases from 0 to 50 (Fig. 6E). In uncomplexed succinate, the ν_s band has a major component at 1397 cm^{-1} and a weak shoulder at 1420 cm^{-1} . Upon Ni(II) addition, the ratio of the $1420\text{ cm}^{-1}/1397\text{ cm}^{-1}$ peak intensities increases without any spectral shift. These spectral changes for succinate are also similar to those observed for simple monocarboxylate ligands. When H_2O is replaced by D_2O , the ν_{as} of weakly complexing carboxylates, such as succinate, is shifted to slightly higher frequencies (Fig. 4B). This effect is similar to changes observed in Ni(II)-free solutions (Fig. 4A).

In tricarboxylate, individual carboxylates are separated by at least two bridging methylene groups (Fig. 2). Similar to succinate, the effect of Ni(II) addition on the infrared spectra of carboxylate is small, even though speciation predictions indicate that $>99\%$ of the ligand is complexed at higher $[M]/[L]$ (Fig. 6F).

3.1.2.4. Nickel complexation with carboxylates that contain alcohol donor groups. The interactions of Ni(II) with the mono-, di-, and tricarboxylic acids are different when alcohol groups are added to these molecules, such as in lactate, malate, and citrate (Fig. 2G-I, Fig. 6G-I). Alcohol groups are poor ligand donors and do not deprotonate at ambient pH conditions, but their presence adjacent to a carboxylate group markedly enhances the degree of metal complex formation (Martell et al., 1997). The alcohol group presumably stabilizes the metal complex by acting as a “supporting” donor group in concert with the adjacent carboxylate. For example, under comparable conditions lactate complexes Ni(II) to a much greater extent than either formate or acetate, and this is clearly shown by the infrared spectra of carboxylates. Addition of Ni(II) modifies spectral features of lactate significantly; the ν_{as} band shifts to higher frequencies by 16 cm^{-1} relative to Ni(II)-free solutions, and two moderately intense, sharp peaks located at 1456 cm^{-1} and 1416 cm^{-1} (Pike et al. (1993) assigned the latter to ν_s) appear to broaden and shift to slightly higher and lower frequencies, respectively. In addition, the $\nu_{\alpha}(\text{C-OH})$ band at 1129 cm^{-1} shifts to slightly lower frequencies upon Ni(II) complexation.

Malate and citrate behave similar to lactate, and a significant fraction of these ligands complex to Ni(II) when present in equimolar concentrations (80% for malate, $\geq 99\%$ for citrate at pH 6). The ν_{as} and ν_s bands broaden considerably and appear to split into two or more components when compared to Ni(II)-free solutions. One component of each absorption band remains relatively unchanged from that of Ni(II)-free solutions, whereas the other shifts to a higher frequency. However, both components of the carboxylate peaks exist at $[M]/[L]$ conditions much higher than required to completely complex the ligands. In addition, the $\nu_{\alpha}(\text{C-OH})$ located near 1095 cm^{-1} in Ni(II)-free solutions, shifts to lower frequencies upon Ni(II) addition. When H_2O is replaced by D_2O , splitting of ν_{as} is pronounced for malonate, malate, and citrate (Fig. 4B). One of the split peaks shifts the same amount that ν_{as} shifts in Ni(II)-free solutions, whereas the other shifts to much higher frequencies. The enhancement of peak splitting in equivalent D_2O solutions confirms that the individual carboxylates within the ligand are experiencing different coordination environments when Ni(II) is added to solution. Infrared spectra reported for Ni(II)-citrate are also similar to those that were observed in solutions con-

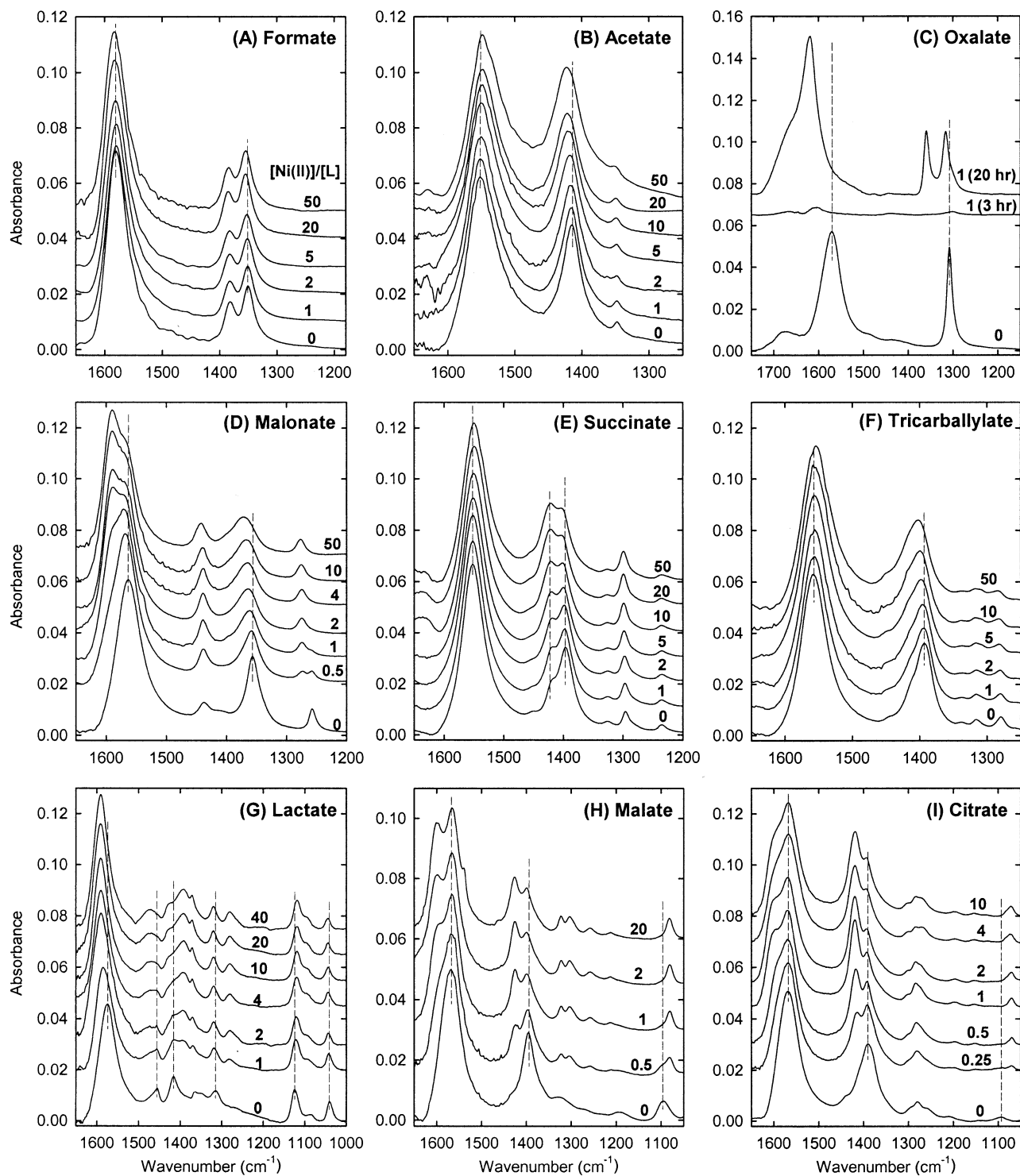


Fig. 6. FTIR spectra of carboxylate ligands as a function of $[M]/[L]$ ratio at a fixed pH. Solution composition: (A) 50 mM formate, pH 5.0; (B) 50 mM acetate, pH 6.0; (C) 25 mM oxalate + 0 mM Ni(II), pH 6.0; precipitate formed in solution containing 2.5 mM oxalate + 2.5 mM Ni(II) at pH 6.0; (D) 50 mM malonate, pH 6.0; (E) 50 mM succinate, pH 6.0; (F) 50 mM tricarballylate, pH 6.0; (G) 25 mM lactate, pH 5.5; (H) 25 mM malate, pH 6.0; (I) 50 mM citrate, pH 6.0. 20 mM carboxylate concentrations used for samples where $[M]/[L] \geq 20$. Spectral intensities of dissolved carboxylates normalized to 50 mM carboxyl moiety.

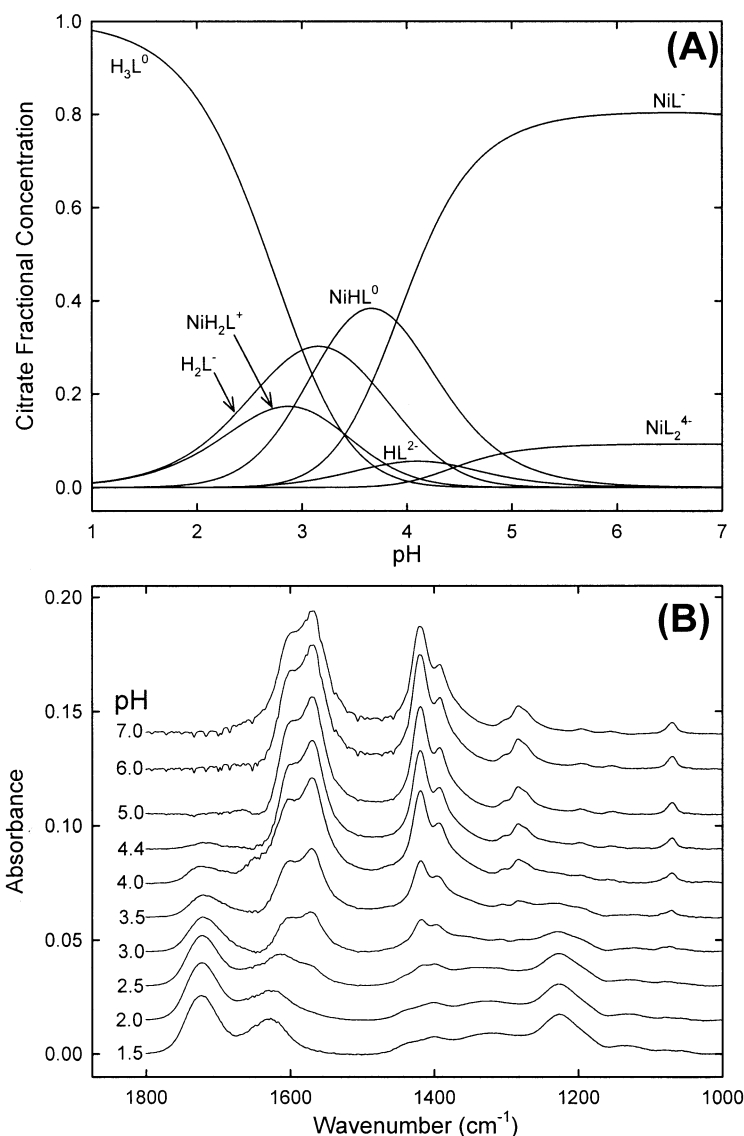


Fig. 7. Effect of pH on the (A) predicted speciation and (B) FTIR spectra of 25 mM citrate in aqueous solutions containing 25 mM Ni(II) and 125 mM NaCl.

taining Ca(II), Mg(II), Mn(II), Co(II), and Zn(II) (data not shown).

3.1.3. Proton titration of nickel-carboxylates

Thermodynamic calculations predict that species with stoichiometries such as NiHL^n and $\text{NiH}_2\text{L}^{n+1}$ begin to account for a significant fraction of total ligand concentration in Ni(II)-containing solutions at low pH. To evaluate the stability and structures of these protonated Ni(II)-carboxylates, infrared spectra were collected for Ni(II)-carboxylate solutions at varying pH but fixed $[\text{M}]/[\text{L}]$. The spectra of these samples (Fig. 7B) in general exhibit the same features as those shown by uncomplexed and Ni(II)-complexed carboxylates discussed earlier (Figs. 3 and 6, Table 1). The principal effect of Ni(II) on infrared proton titrations of the carboxylates is a lowering of the pH where ν_{as} and ν_{s} bands are replaced by $\nu(\text{C}=\text{O})$ and $\nu(\text{C}-\text{OH})$. This is consistent with a

competition between Ni(II) and protons for the carboxylate donor groups. For example, speciation calculations for Ni(II)-citrate solutions (25 mM citrate, 25 mM Ni(II), $\mu = 0.2$ mol/L) predict that 50% of citrate should be present as a species with stoichiometry NiHL^0 or NiH_2L^+ between pH 3–4 (Fig. 7A). Infrared spectra of these samples do not exhibit new features when compared to the Ni(II)-citrate and Ni(II)-free citrate solutions (Figs. 6I and 3I, respectively). However, it should be noted that the Ni(II)-carboxylate complex does not decompose completely (split ν_{as} persists with the same ratio for both components) as the pH of Ni(II)-citrate solutions is lowered (pH > 2.5). Instead its concentration decreases and the concentration of protonated carboxylate species increases. This indicates that either the measured stability constants are over-predicting the concentration of these species or that their characteristic spectral features are not markedly different from other citrate species.

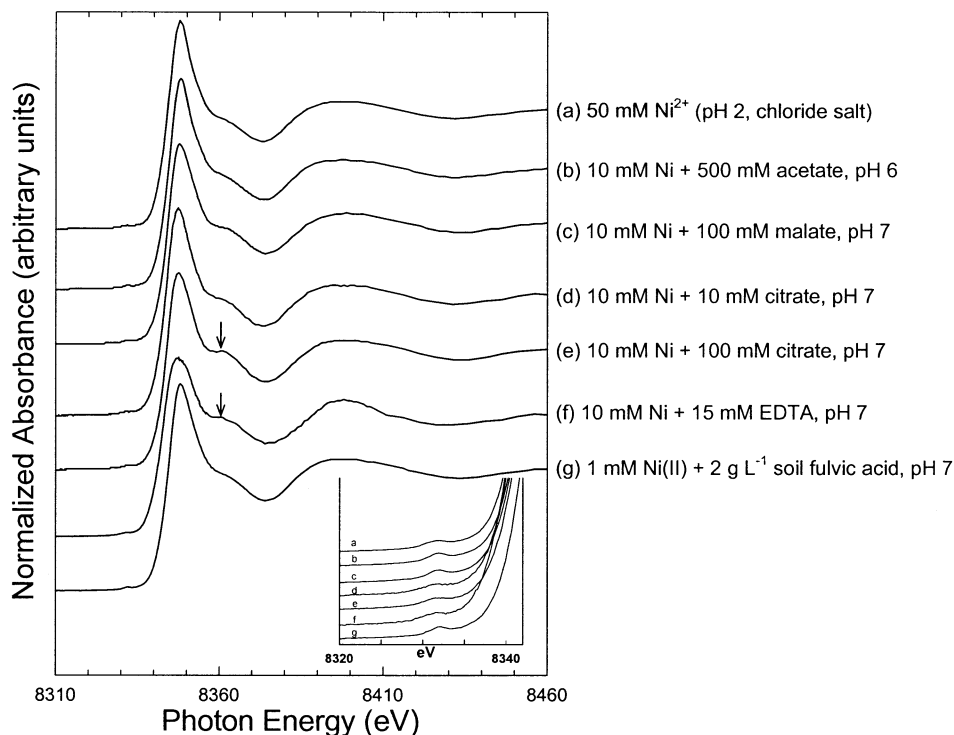


Fig. 8. Representative Ni *K*-edge XANES spectra for selected aqueous Ni(II)-carboxylate solutions. Inset shows close-up of pre-edge $1s \rightarrow 3d$ transition. Solution compositions listed on figure. Predominant species predicted from reported stability constants: (a) $\text{Ni}(\text{H}_2\text{O})_6^{2+}$, (b) $\text{Ni}(\text{acetate})^+$ and $\text{Ni}(\text{acetate})_2^0$, (c) $\text{Ni}(\text{malate})^0$, (d) $\text{Ni}(\text{citrate})^-$, (e) $\text{Ni}(\text{citrate})_2^{4-}$, (f) $\text{Ni}(\text{EDTA})^{2-}$, (g) not available. Arrows indicate broadening of first oscillation.

3.2. XAFS Spectra

Ni *K*-edge XAFS spectroscopy measurements were carried out to evaluate the structure and bonding environment of Ni in aqueous solutions containing low-molecular-weight aliphatic carboxylates and fulvic acid. Samples for X-ray studies were selected on the basis of speciation calculations. Solution conditions were selected where Ni(II)-carboxylate species of a desired stoichiometry, such as NiL and NiL_2 , were predicted to predominate. For weakly complexing ligands, this necessitated the use of low $[\text{M}]/[\text{L}]$. In addition, X-ray spectra were collected for solutions containing strongly complexing amino-carboxylates (INTA) and ethylenediaminetetraacetic acid (EDTA) to evaluate their influence on the XANES and EXAFS spectra of Ni(II).

3.2.1. XANES spectra of Ni(II)-carboxylate complexes

The XANES spectra of Ni exhibit a distinct weak pre-edge feature and a strong main absorption edge feature, which are sensitive to the oxidation state and coordination environment of Ni (Fig. 8). The pre-edge feature arises from electronic transitions of Ni $1s \rightarrow 3d$ orbitals. Although these transitions are forbidden for centrosymmetric octahedral complexes, distortions in symmetry allow for some $d - p$ orbital mixing, which enhances the probability of $1s \rightarrow 3d$ transitions (Kosugi et al., 1986; Colpas et al., 1991; Galois and Calas, 1993; Feth et al., 2003). The pre-edge feature is expected to be more intense in noncentrosymmetric molecules, such as tetrahedral and square

pyramidal complexes (Colpas et al., 1991). Square planar complexes are differentiated from octahedral complexes by the presence of a pre-edge feature near ~ 8338 eV, which is due to $1s \rightarrow 4p_z$ transitions (Kosugi et al., 1986; Colpas et al., 1991); the lack of this feature in spectra collected here indicates that aqueous Ni complexes with carboxylic and fulvic acids are not square planar. The intensity of the pre-edge feature of Ni in all carboxylate solutions is weak and is similar to that of hydrated $\text{Ni}(\text{H}_2\text{O})_6^{2+}$ species (e.g., dissolved salts of chloride, nitrate, perchlorate), which suggests that Ni is octahedral and its polyhedron does not deviate significantly from octahedral geometry with changes in the identity of the complexing ligand(s).

The main absorption edge (white line), corresponding to $1s \rightarrow 4p$ transitions, is similar for all samples examined, indicating that Ni is present in the +II oxidation state. Solutions predominantly containing either $\text{Ni}(\text{EDTA})^{2-}$ or $\text{Ni}(\text{citrate})_2^{4-}$ (predicted by speciation calculations) exhibit slight broadening of a feature on the high-energy side of the white line. However, these two solutions are unique in that they are the only samples examined in which Ni(II) is coordinatively saturated by non-aquo ligands. This change, although minor, indicates some modification of the electronic and coordination environment of Ni(II). The postedge features for the Ni(II)-carboxylate and Ni(II)-fulvic acid complexes, which arise from single- and multiple-scattering processes involving ejected photoelectrons (Koningsberger and Prins, 1988), are similar to hexaquo Ni^{2+} . This indicates that the inner coordination geometry of the Ni(II)

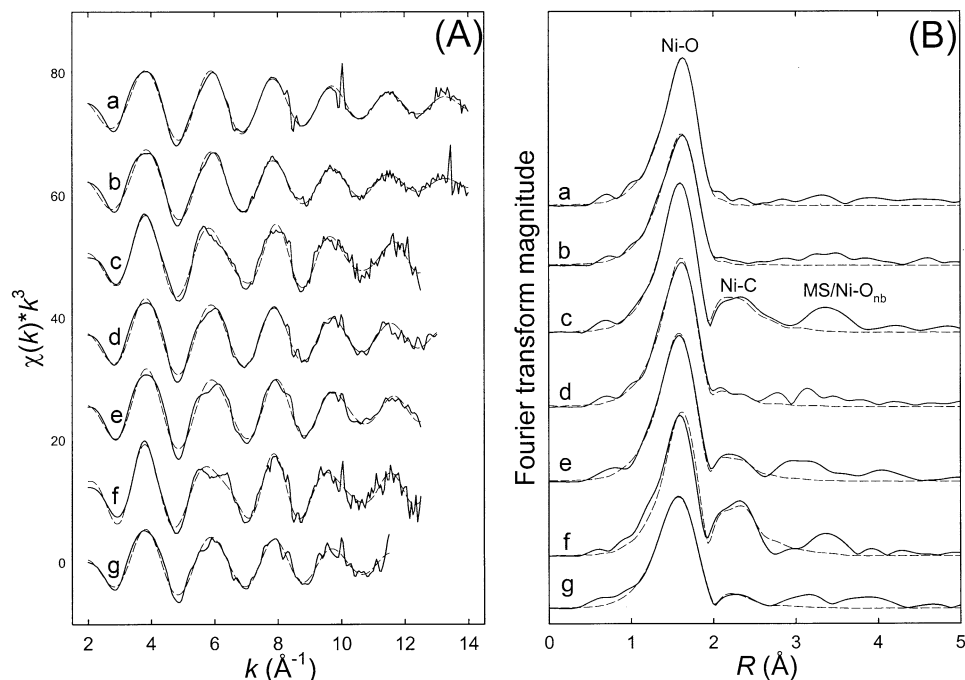


Fig. 9. Representative Ni *K*-edge EXAFS spectra (solid lines) and spectral fits (dotted lines) of aqueous Ni-carboxylate and Ni-fulvic acid complexes. The normalized k^3 -weighted χ functions are shown in panel A. The radial structure functions (RSFs) are shown in panel B. Spectra include (a) 50 mM NiCl_2 at pH 2, (b) 10 mM Ni + 500 mM acetate at pH 6, (c) 5 mM Ni + 40 mM oxalate at pH 6, (d) 10 mM Ni + 10 mM citrate at pH 7, (e) 10 mM Ni + 100 mM citrate at pH 7, (f) 10 mM Ni + 15 mM EDTA at pH 7, and (g) 1 mM Ni + 2 g L^{-1} fulvic acid at pH 7.

ion is not significantly altered upon complexation by these ligands.

3.2.2. EXAFS spectra of Ni(II)-carboxylate and Ni(II)-fulvate complexes

EXAFS spectra were collected for hexaquo Ni^{2+} , Ni(II) complexes with weakly- and strongly-binding carboxylates, and Ni(II) solutions containing fulvic acid (Fig. 9). The extracted EXAFS spectra of all of these samples, except those of strongly complexing carboxylates, are characterized by symmetrical oscillations (Fig. 9A). In contrast, EXAFS spectra for Ni(II) complexes with strongly-binding ligands, such as oxalate and EDTA, contain additional structure that leads to asymmetry or splitting in the oscillation near 6 \AA^{-1} . This suggests a significant difference in the coordination geometry of Ni(II) in solutions containing weakly and strongly complexing carboxylates. The radial structure functions of the EXAFS spectra show an intense peak at 1.65 \AA (uncorrected for phase) and small peaks between 2.0 and 2.5 \AA (uncorrected for phase). These peaks are related to the scattering from the first-shell O atoms around Ni(II) and second-shell C, N, or O atoms, respectively. Although additional peaks are also observed in most RSFs between 3 and 4 \AA (uncorrected for phase), they are greatest for complexes that exhibit a "rigid" structure, such as in Ni(II)-oxalate, -NTA, and -EDTA complexes. Although these peaks could be fit with a combination of multiple-scattering (MS) and single-scattering paths, solutions to these fits are not unique. Thus, no structural information may be derived from these fits.

3.2.2.1. First-shell Ni-O. Fitting the first-shell peak at 1.65

\AA using the theoretically derived phase and amplitude functions indicates the presence of 5.4 – 6.6 O atoms located at 2.03 – 2.06 \AA . These results are similar to those previously reported for a number of aqueous and solid phase Ni(II) species and are consistent with the NiO_6 octahedron (Sandstrom, 1979; Scheidegger et al., 1996; Xia et al., 1997; Trivedi et al., 2001; Nachttegaal and Sparks, 2003).

3.2.2.2. Second-shell Ni-C/N/O. Smaller peaks at *R* values between 2.0 and 2.5 \AA arise from either spectral noise or scattering from distant C, N, or O atoms that may exist at higher *R* in all Ni(II)-carboxylates examined. Obtaining unequivocal structural information from spectral fits of these small peaks is rather difficult, especially for weakly complexing carboxylates. This is because lighter elements, such as C and N in organic molecules, are weak scatterers, and larger numbers of these atoms and/or rigid structures (e.g., porphyrin rings surrounding metal ion) are required to definitively demonstrate their presence in the second or higher shells. It should also be noted that the error associated with coordination number estimates from EXAFS is large. As a practical measure, we have chosen only to report second-shell structural parameters when fits indicate $\text{CN}_{\text{Ni-C}} \geq 2$ and standard deviations on $\text{CN}_{\text{Ni-C}} < 50\%$. When $\text{CN}_{\text{Ni-C}} < 2$, the only structural information we assume is that $0 \leq \text{CN}_{\text{Ni-C}} \leq 2$. After correcting for phase, these peaks between 2.0 and 2.5 \AA in RSF give a Ni-C/N bond distance of 2.82 – 2.86 \AA for the Ni(II)-carboxylate complexes, regardless of the complexing carboxylate. The question is how many C atoms are present at this distance? Information on the number of scatterers and their distances is required to

identify the structures of the complexes. A detailed spectral analysis of strongly and weakly complexing carboxylates is presented below.

Second-shell features in the RSFs of Ni(II) solutions containing strongly complexing ligands (e.g., oxalate, malate, citrate, NTA, EDTA) are intense relative to the spectral noise. Ni(II)-chelating agents, such as aminocarboxylic acids, form "rigid" structures with several second-shell carbon atoms held tightly in fixed positions and thus exhibit intense backscattering in the second-shell region of the RSF. The second-shell peaks for Ni(II)-EDTA and Ni(II)-NTA complexes are more intense than the other carboxylate ligands considered in this study (Fig. 9B trace f). Fits of these spectral features indicate a coordination number of $CN_{Ni-C} = 6.6$ for a Ni(II) atom complexed by NTA, consistent with a 1:1 complex where all three carboxyls and the bridging amino group coordinate Ni(II) (predicted $CN_{Ni-C} = 6$). Ni(II) complexed by EDTA showed a $CN_{Ni-C} = 9.4$, consistent with the formation of a 1:1 complex where Ni(II) is coordinated by all four carboxyls and the two bridging amino groups (predicted $CN_{Ni-C} = 10$). Similarly, the spectral fitting of Ni(II)-oxalate solutions ($[M]/[L] = 1/8$) shows a $CN_{Ni-C} = 5.4$ for the second shell, which agrees closely with the predominance of 1:2 complexes predicted from speciation calculations. If Ni(II) forms inner-sphere coordination complexes with both carboxyl groups from each oxalate (bidentate) participating in the complex, then the second shell should have 4 C atoms. As discussed earlier, Ni(II)-oxalate precipitates even in dilute solutions, and unequivocal identification of the structure of the solution complex and the precipitate is not possible. Ni(II)-malate solutions ($[M]/[L] = 1/10$) indicate $CN_{Ni-C} \sim 3$. The malate structure has an alcohol group with two carboxylates, and the fit-derived structural parameters are consistent with the predicted predominance of a 1:1 Ni(II)-malate complex wherein the metal complexes with either two or three of the donor groups.

EXAFS spectra were also collected for Ni(II)-citrate in three different conditions: two solutions at pH 7.0 with $[M]/[L] = 1$ and 10, and one at a pH of 3.5 with $[M]/[L] = 10$. Spectral fitting of solutions at neutral pH indicate a $CN_{Ni-C} \sim 2.7$ and 4.1 for $[M]/[L] = 1$ and 10, respectively. These parameters are consistent with the predicted predominance of 1:1 and 1:2 complexes in these solutions, respectively. Like malate, Ni(II) forms inner-sphere complexes with either two or three donor groups within the structure of each complexed ligand molecule. This result also implies that one or more of the four donor groups is not participating in direct metal coordination. These groups may be uncoordinated or complexed via outer-sphere interactions. This agrees with the reported crystal structure of a Ni(II)-citrate solid precipitated from aqueous solution at pH 5.0. In this solid, Ni(II) is coordinated by the protonated alcohol, the central carboxylate, and one of the two terminal carboxylates (Baker et al., 1983). At pH 3.5, the spectral fit of Ni(II)-citrate solution shows a CN_{Ni-C} of 2.0, which is a decrease from the value of 4.1 determined at neutral pH. This is consistent with the predicted dissociation of the 1:1 and 1:2 complexes upon lowering pH. This is in agreement with the infrared spectral analysis discussed earlier.

For hexaquo Ni^{2+} species and Ni(II) solutions containing weakly binding ligands (acetate, succinate, and tricarboxylate), spectral intensity between 2 and 3 Å is small and cannot be

distinguished from background spectral noise. Attempts to fit second-shell features yield $CN_{Ni-C} < 2$ (with standard deviations on this estimate of nearly 100% or more). As a result, no structural information for second-shell atoms is provided for these solutions. As mentioned in the experimental section, this result does not imply that carbon atoms are not present in the second shell, but rather that $0 \leq CN_{Ni-C} \leq 2$. This result suggests that Ni(II) is either uncomplexed, complexed via outer-sphere mechanisms, or coordinated via a single carboxylate group in a monodentate fashion.

3.2.2.3. EXAFS of Ni(II)-soil fulvic acid solutions. Complexation of Ni(II) with a naturally occurring biopolymer, fulvic acid, was examined for a range of conditions: $[M]/[L] = 1$ mM/2 g L⁻¹ and 1 mM/4 g L⁻¹; pH 5.5–8.5 (Table 2, Fig. 9). The first peak in the RSF is around 1.65 Å, which corresponds to the scattering from first-shell O atoms around Ni(II). The intensity of peaks between 2 and 2.5 Å is not markedly higher than the level of spectral noise observed at higher *R* space. Nonetheless, second-shell EXAFS analysis was carried out for comparison with Ni(II) complexes formed with low-molecular-weight carboxylates. Two-shell spectral fits indicate a higher degree of variability in Ni-C bond lengths (2.80–2.87 Å) and coordination number (1.8–3.5). These structural parameters agree well with previous reports (Xia et al., 1997; Nachttegaal and Sparks, 2003).

4. DISCUSSION

Carboxylates can interact with Ni(II) in different ways as shown in Figure 1, and infrared and X-ray spectroscopy can be used to identify the structures of metal-carboxylate complexes. Important clues from X-ray spectral data of Ni(II) include changes in the XANES spectra, which provide information on distortions in the Ni(II) octahedron and XAFS spectral features indicative of scattering from second-shell C atoms, which yield information on the distance and number of neighboring C atoms surrounding Ni(II). Similarly, the coordination environment of the metal-ligand complexes can be predicted from vibrational spectra provided that changes in the spectral features of the carboxylate groups as a function of the following variables are understood: i) protonation, hydration, and metal complexation; ii) electron delocalization within the carboxylate-metal complex (covalent or ionic character of the metal-carboxylate bond); iii) symmetry variations associated with complex formation or solvation (e.g., deviation from C_{2v} for COO^-); iv) Ni-O-C bond angle variations (linear vs. bent configuration); v) chemical state of individual carboxylates within the structure of polycarboxylates resulting from H-bonding and metal complexation; and vi) vibrational coupling.

The vibrational spectra of crystalline metal carboxylates (for which the structural analysis is available) and theoretical investigations can be used to elucidate the influence of the above mentioned effects on infrared spectra. While crystal structure analysis of several inorganic phases is available, such an analysis of metal carboxylates, especially for hydrated salts, is not extensive. Because H-bonding can significantly alter the vibrational bands of carboxylates, the location of H atoms and the lengths of H-bonds in crystals are necessary for evaluating the influence of metal complexation and H-bonding on the vibrational spectra of metal carboxylates. Although some structural

Table 2. Best-fit structural parameters derived from EXAFS analysis^a.

Sample	pH	μ^b (M)	Predominant species ^c	Ni-O Shell			Ni-C Shell			ΔE_o (eV)	% res
				CN	R (Å)	σ^2 (Å ²)	CN	R (Å)	σ^2 (Å ²)		
Ni(II)-Carboxylate complexes											
50 mM Ni(H ₂ O) ₆ ²⁺ (NO ₃ salt)	2.0	0.15	Ni(H ₂ O) ₆ ²⁺	6.0	2.05	0.005				3.10	5.7
10 mM Ni + 500 mM acetate	6.0	0.44	NiL ⁺ (40%), NiL ₂ ⁰ (44 %), Ni(H ₂ O) ₆ ²⁺ (16%)	6.4	2.05	0.006				3.66	5.8
5 mM Ni + 40 mM oxalate	6.0	0.10	NiL ₂ ²⁻	5.8	2.04	0.004	5.4	2.82	0.005	2.16	3.9
10 mM Ni + 100 mM succinate	7.0	0.28	NiL ⁺ (60%), Ni(H ₂ O) ₆ ²⁺ (40%)	6.2	2.05	0.006				3.34	5.8
10 mM Ni + 100 mM tricarallylate	7.0	0.56	NiL ⁻	6.4	2.05	0.007				3.52	6.4
10 mM Ni + 100 mM malate	7.0	0.25	NiL ⁰	6.0	2.04	0.006	3.1	2.83	0.009	3.38	4.5
10 mM Ni + 10 mM citrate	7.0	0.034	NiL ⁻	6.2	2.04	0.005	2.7	2.84	0.008	2.82	6.5
10 mM Ni + 100 mM citrate	7.0	0.51	NiL ₂ ⁴⁻	6.2	2.03	0.005	4.1	2.83	0.007	2.52	4.8
10 mM Ni + 100 mM citrate	3.5	0.21	NiHL ⁰ (55%), NiL ⁻ (22%), NiH ₂ L ⁺ (15%), Ni(H ₂ O) ₆ ²⁺ (6%)	6.1	2.04	0.006	2.0	2.83	0.008	3.51	4.1
10 mM Ni + 10 mM NTA	7.0	0.030	NiL ⁻	5.7	2.05	0.005	6.6	2.84	0.007	2.74	5.9
10 mM Ni + 15 mM EDTA	7.0	0.082	NiL ₂ ²⁻	5.4	2.05	0.004	9.4	2.86	0.007	3.37	8.1
Nickel acetate tetrahydrate (s)			NiL ₂ (H ₂ O) ₄ (solid)	6.3	2.06	0.005				4.56	7.4
Ni(II)-Fulvic acid complexes											
1 mM Ni + 2 g/L fulvic acid	5.5	n/a		5.4	2.04	0.005	3.5	2.80	0.011	2.62	5.3
1 mM Ni + 2 g/L fulvic acid	7.0	n/a		5.5	2.04	0.006	3.1	2.85	0.009	2.58	2.8
1 mM Ni + 2 g/L fulvic acid	8.5	n/a		5.6	2.04	0.006	1.8	2.84	0.007	2.08	5.1
1 mM Ni + 4 g/L fulvic acid	7.0	n/a		6.6	2.03	0.007	2.1	2.87	0.006	2.96	4.2

^a CN = coordination number ($\pm 20\%$; O'Day et al., 1994). R = interatomic distance (± 0.02 ; O'Day et al., 1994). σ^2 = Debye-Waller factor. ΔE_o = phase shift relative to 8345 eV. % res = residual error in R space from 0.9–2.8 Å.

^b Calculated ionic strength of solution analyzed. No estimates of ionic strength were made for fulvic acid solutions since the molar concentration, structure, and charge of the fulvic acid molecules are unknown.

^c Predominant Ni(II) species or mixture of species predicted from thermodynamic speciation calculations for conditions listed (Martell et al., 1997). When only a single species is listed, calculations predict that it represents $>90\%$ of $[\text{Ni(II)}]_{\text{tot}}$.

analysis of Ni(II)-acetate, Ni(II)-malonate, and Ni(II)-citrate is available, detailed infrared spectral analysis of these phases with respect to hydrogen bonding is missing (Downie et al., 1971; Baker et al., 1983; Nicolai et al., 1998; Ruiz-Pérez et al., 2000). Although ab initio and semi-empirical calculations can help in the evaluation of infrared spectra, the spectral variations recorded for aqueous carboxylates in the absence and presence of Ni(II) are too small to predict using these approaches (<35 cm⁻¹ for all examined ligands). In addition, calculations for hydrated species with one or two shells of solvation involve large clusters of atoms, which are almost impossible to handle with methods that can model solvation more accurately (e.g., ab initio molecular dynamics simulations). Although calculations of gas-phase species with one or two water molecules can be used in the identification of vibrational bands, predictions for small energy shifts cannot be made accurately for the reasons discussed above (Axe and Persson, 2001).

Several researchers studying aqueous and adsorbed metal-carboxylate complexes use an empirical rule derived from observations on crystalline metal acetate complexes to identify the structure of metal-carboxylate complexes from infrared spectra (Deacon and Phillips, 1980). This empirical rule suggests that monodentate coordination in crystalline solids is accompanied by a significant increase in ν_{as} and a decrease in ν_{s} when compared to the vibrational bands of the uncomplexed carboxylate. As a result, $\Delta\nu$ (separation between ν_{as} and ν_{s}) is greater than 200 cm⁻¹, which is significantly larger than the separation of 164 cm⁻¹ observed for the outer-sphere (H-bonding) interactions in the sodium acetate solid. In con-

trast, bidentate chelate coordination is typically accompanied by a large decrease in ν_{as} and an increase in ν_{s} , with the resulting $\Delta\nu$ values being less than 105 cm⁻¹. Bidentate bridging coordination is usually accompanied by minimal changes in $\Delta\nu$ that result from either small changes in ν_{as} and ν_{s} , or larger changes in each band that occur in the same direction and are of similar magnitude. Because this empirical relationship is derived from solid-state metal acetate complexes, its application to metal-carboxylates in aqueous solutions and at interfaces, and to polycarboxylate-metal complexes is questionable. Although energy shifts discussed above are valid for the suggested coordination geometries, their magnitudes tend to be different because of several variables, discussed above, which can influence vibrational band shifts. Furthermore, some of the vibrational bands, such as ν_{s} , are strongly coupled with those of other groups, such as C-C and C-H, and the contribution of the ν_{s} is distributed over several peaks (Quilès et al., 1999).

Major changes in the infrared spectra of carboxylates are associated with protonation of the ligand, because the inequality of the two CO bonds increases and involves significant changes in the force constants of the carboxylate group. The protonated C-OH bond lengthens whereas the double bond character in the unbound C=O strengthens. This leads to a large energy separation between C-OH and C=O vibrations. When a deprotonated carboxylate interacts with metals in solution, the relative changes in the spectra of the carboxylate group depend on the bond angles, modifications in the hydration of the carboxylate during complex formation, and sharing of the electron density between the carboxylate and metal ion

(i.e., covalent or ionic character of the bond). Because changes in the vibrational bands are small for all carboxylates examined in this investigation, variations in force constants caused by Ni(II) complexation and hydration are considered small. Hence, we attempt to characterize the strength of metal-carboxylate interactions from relative changes in the spectra of Ni(II)-containing and Ni(II)-free carboxylate solutions. Wherever possible, attempts were made to combine infrared and XAFS spectral information to understand the nature of Ni(II)-carboxylate interactions.

4.1. Structure and Coordination of Ni(II)-Carboxylate Complexes

The coordination environment of Ni(II)-carboxylates is discussed under two different groups based on their infrared and X-ray spectral features. The first group includes monocarboxylates and long-chain polycarboxylates, where separation of individual carboxylate donor groups by multiple bridging methylene groups inhibits simultaneous coordination of Ni(II) by multiple carboxylate moieties (Martell et al., 1997). The second group includes ligands that complex Ni(II) to a greater extent, and a priori structural considerations support simultaneous coordination of a single Ni(II) ion by multiple donor groups (Bell, 1977).

4.1.1. Coordination of Ni(II) with acetate, formate, succinate, tricarballylate

XANES and EXAFS studies of Ni(II) complexation with this class of carboxylates indicate that Ni(II) is octahedrally coordinated by O atoms with minimal distortion (similar to aqueous $\text{Ni}(\text{H}_2\text{O})_6^{2+}$), and significant scattering from second-shell C atoms of the carboxylate is absent. Based on these results, formation of a bidentate chelate complex with a single carboxylate group, and simultaneous coordination of Ni(II) by multiple carboxylate moieties within a single ligand molecule can be ruled out. Because the bond distances of Ni-O and C-O are ~ 2.04 Å (measured from EXAFS) and ~ 1.27 Å (Deacon and Phillips, 1980), respectively, octahedral Ni(II) cannot form a bidentate chelate with a single carboxylate. If the Ni(II) octahedron is distorted to increase the distance between Ni and C and accommodate the C atom, the pre-edge intensity should increase significantly in the XANES spectra, and scattering from the second-shell C atoms should be greater in the EXAFS. These spectral variations are absent in all Ni(II)-carboxylate complexes examined.

The vibrational bands of this class of carboxylates are not altered significantly when Ni(II) is added to solutions. The presence of Ni(II) in carboxylate solutions causes a small decrease (or no change) in ν_{as} and a small increase in ν_{s} when compared to Ni(II)-free solutions. Monodentate coordination in crystalline Ni(II)-acetate has been shown to exhibit similar infrared spectral trends in some studies, but reports vary significantly from different studies, thus calling into question the utility of making comparisons between solution and solid-phase data (Edwards and Hayward, 1968; Deacon and Phillips, 1980; Bickley et al., 1990). The small variations observed for aqueous solutions can be caused by interactions of Ni(II) with the carboxylate either through weak inner-sphere or outer-

sphere complex formation, which do not change the force constants of the carboxylate moiety. Weak inner-sphere coordination can be thought of as a flexible bond where the Ni(II) ion is not held in a fixed position with respect to the COO^- group (Fig. 10). By allowing the metal ion to adopt a variety of orientations, the equivalence of the two C-O bonds is largely maintained. Small changes or reorganization of solvated water at the carboxylate group can also contribute to small spectral changes observed. An alternative explanation is that only a small fraction of carboxylates are complexed with Ni(II) when compared to those estimated from thermodynamic speciation.

The polycarboxylates of this class also exhibit small shifts in the ν_{as} and ν_{s} bands for Ni(II)-carboxylate solutions. The ν_{as} band does not split (unlike other carboxylates discussed in the next section), and the ν_{s} splits (weak for tricarballylate when compared to succinate). This splitting is caused by changes in the vibrational coupling associated with Ni(II) complexation. Based on the observed weak spectral shifts, the interactions between Ni(II) and the carboxylate are considered to be similar to those of monocarboxylates discussed above. These small spectral shifts may also indicate that the Ni(II)-complexed species contain both free and coordinated carboxylate groups, and the molar absorptivities of the IR bands originating from the coordinated groups might be lower than those of the free groups (Kubicki et al., 1996; Axe and Persson, 2001). For example, if Ni(II) only coordinates to a single carboxylate group in tricarballylate, then two-thirds of the carboxylate groups still remain uncoordinated even in solutions where 100% of the ligand molecules are complexed by the metal.

4.1.2. Coordination of Ni(II) with lactate, oxalate, malate, malonate, citrate

Pre-edge features in XANES spectra of these samples are similar to that of $\text{Ni}(\text{H}_2\text{O})_6^{2+}$, indicating that Ni(II) in complexes with these ligands is octahedral as well. However, small changes in the main absorption edge of the XANES spectra of citrate indicate that scattering from second shells is different than in hexaquo Ni^{2+} . The scattering from second-shell C atoms in EXAFS spectra (in RSF; Fig. 9) also indicates interactions of Ni(II) with at least one and, perhaps, multiple donor groups of the carboxylates (Table 2). Because the Ni-C distances are estimated to be $2.84 (\pm 0.02)$ Å in all of the Ni(II)-carboxylates studied and the Ni-O-C bond is not linear (around 110°), the results suggest that the Ni(II)-carboxylate structure is similar in all of these molecules (Table 2). It is surprising to see that the Ni-C distances in malate and citrate are the same as those found in Ni(II)-chelating ligands, such as oxalate, EDTA, and NTA. To maintain similar Ni-C distances (or Ni-O-C bond angle) in malate and citrate, another functional group such as the alcohol or another carboxylate (such as in oxalate) has to approach the coordination sphere of Ni(II) (Fig. 10).

The infrared spectra also show significant changes when Ni(II) is added to these carboxylate-containing solutions (when compared to the previous category). Important changes include: i) splitting of the ν_{s} and ν_{as} bands, which may be caused by changes in vibrational coupling, presence of two or more molecularly distinct carboxylate groups, or changes in the symmetry of the COO^- resulting from Ni(II) complexation; ii)

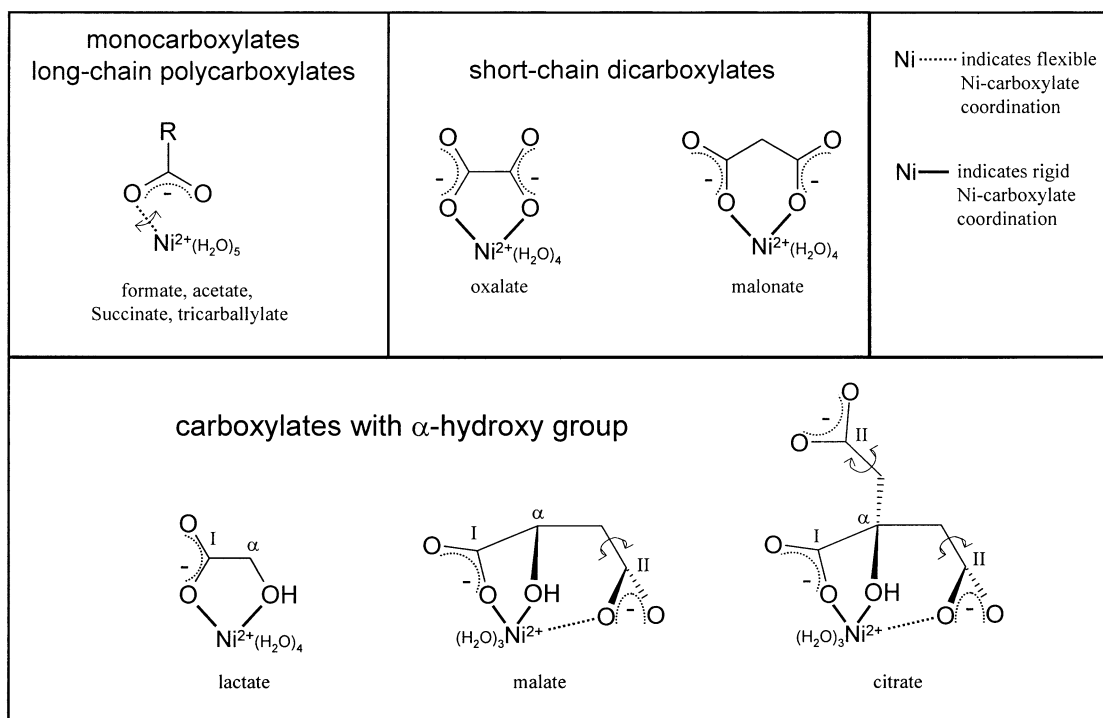


Fig. 10. Proposed structures for 1:1 Ni(II)-carboxylate complexes. Dashed coordination bonds indicate “flexible” bonds where the Ni atom is held such that the distance to the unbonded oxygen atom is not much greater than the distance to the bonded oxygen atom. Solid coordination bonds indicate “rigid” bonds where the distance between Ni and the unbonded oxygen atom is significantly longer than the distance to the bonded oxygen atom.

significant shift of the ν_{as} bands to higher energy when compared to those of the previous class of carboxylates; and iii) increase in the intensity of the high-energy component of the ν_s band.

The energy difference between the two components of the ν_{as} and ν_s bands observed with increases in Ni(II) concentration is $\sim 31\text{ cm}^{-1}$ for both malate and citrate. This trend is similar to that of Ni(II)-oxalate, but the shift is much higher for the latter ($\sim 50\text{ cm}^{-1}$). The centroid of ν_{as} and ν_s shifts to higher energy for all these ligands (with the highest value for oxalate), which may be caused by variations in the charge distribution within the carboxylate group when complexed by Ni(II). Because both ν_{as} and ν_s are shifting to higher energy by the same magnitude, the CO groups in these carboxylates are similar to the uncomplexed carboxylate but exhibit shorter CO distance and possess more partial double bond character on each CO. Differences in the strengths of interactions are responsible for variation in the relative shifts of oxalate, malonate, malate, and citrate. Combination of EXAFS and infrared data indicates that Ni(II) forms inner-sphere complexes with these ligands, and the coordination geometries are similar.

The splitting of ν_s and ν_{as} bands of selected carboxylates may indicate the presence of both complexes and uncomplexed ligands in solution (e.g., L^- , NiL^+) or variations in the coordination environment of individual carboxylates within the polycarboxylate ligand structure (e.g., one metal-coordinated group and one or more uncoordinated groups). Because these spectral features are also present at much higher Ni(II) concentrations than is required to complex all of the ligand, the latter

hypothesis is proposed for all these ligands. Although vibrational coupling cannot be ruled out as an explanation, vibrational coupling of ν_{as} with other groups is small when compared to the ν_s (Dobson and McQuillan, 1999; Axe and Persson, 2001). Hence the spectral splitting of ν_{as} is probably caused by nonequivalent carboxylate groups (note that such a splitting is not found in the case of succinate and tricarballylate of the first group). Because the position of one of the split peaks of ν_{as} remains unchanged for malate and citrate when compared to their uncomplexed species, it is hypothesized that some of the carboxylate groups are either not coordinated to Ni(II) or are coordinated in a more flexible fashion (Fig. 10).

A small shift in the $\nu_{\alpha}(\text{C-OH})$ to lower frequencies observed upon Ni(II) addition to lactate, malate, and citrate solutions suggests that the alcohol group participates in Ni(II) coordination. The alcohol group retains its proton during Ni(II) coordination; deprotonation would be expected to cause a much larger shift in the opposite direction. This result is also consistent with the observed crystal structure of a Ni(II)-citrate solid precipitated under conditions similar to those examined here (Baker et al., 1983).

For malonate, the energy difference between the split components of ν_{as} that originate because of Ni(II) interactions is $\sim 25\text{ cm}^{-1}$, whereas the ν_s shifts to high energy by only 15 cm^{-1} . Because the two carboxylate groups are chemically equivalent in malonate, it is difficult to ascribe peak splitting to different modes of coordination. Although $\sim 100\%$ of malonate is predicted to be complexed when $[M]/[L] > 4$, the spectrum continues to shift as $[M]/[L]$ is further increased up to 50, the

highest ratio examined. This may indicate that speciation calculations are incorrect and significantly over-predict the degree of Ni(II) complexation. An alternative explanation is that two distinct complexes with 1:1 stoichiometry coexist in solution, one inner-sphere oxalate-like bidentate complex as shown in Figure 10, and one outer-sphere complex with spectral features similar to uncomplexed malonate (Rudolph et al., 1997; Rudolph et al., 1999). If we assume that the high- and low-frequency components of ν_{as} are due to the former and latter complexes, respectively, then the spectral trends indicate that a shift in species distribution occurs when $[M]/[L]$ is increased. The bidentate structure agrees with the X-ray crystal structure refinement recently reported for a Ni(II)-malonate solid precipitated in alkaline solution (Ruiz-Pérez et al., 2000).

A combination of X-ray and infrared spectroscopy studies of this class of carboxylates indicates that Ni(II) forms inner-sphere chelate-type complexes with carboxylate and hydroxyl groups (Fig. 10). For chelate formation, the hydroxyl may be a better ligand than the second carboxylate group because of its proximity. While monocarboxylates and polycarboxylates discussed in the previous category may not form such structures because of steric considerations, the OH group in lactate, malate, and citrate can promote the interactions between carboxylates and Ni(II).

4.2. Soil Fulvic Acid Complexes

X-ray spectral data of Ni(II)-soil fulvic acid solutions can be compared with data for Ni(II)-carboxylates discussed above to characterize Ni(II)-fulvic acid interactions. Infrared studies could not be conducted for these solutions, because high concentration of fulvic acid is required to collect ATR-FTIR spectra of fulvic acid (it follows that extremely high Ni(II) concentration is required to saturate a majority of carboxylate groups). The EXAFS spectra for Ni(II)-fulvic acid complexes indicate Ni-C distances of $\sim 2.84 \text{ \AA}$, but the range of estimates for the coordination number of second-shell C is large (1.8–3.5). Although these parameters are consistent with inner-sphere Ni(II) coordination by one or more carboxylate groups in the fulvic acid structure, they are tenuous estimates at best. Hence it is difficult to predict whether fulvic acid forms complexes similar to that of monocarboxylate and long-chain polycarboxylate ligands of the first class, or chelates of the second class. The lack of intense second-shell backscattering, however, indirectly suggests that the complexes similar to the first class are more likely.

5. CONCLUSION

A combination of molecular information from the infrared and X-ray spectroscopy studies of Ni(II) carboxylates with results from previous thermodynamic studies refines our understanding of Ni(II)-carboxylate interactions in aqueous solution. A summary of these findings indicates the following:

- 1) Ni(II) forms weak complexes with monocarboxylates and polycarboxylates where individual carboxylate groups are separated by two or more bridging methylene groups. The structural environment and speciation of these Ni(II)-carboxylate solutions are difficult to predict using the infrared and X-ray spectroscopy information alone.

- 2) Carboxylates that contain either multiple closely-spaced carboxylate groups or an alcohol donor adjacent to one of the carboxylate groups interact more strongly with Ni(II) and form chelate-type structures. Based on the spectral information presented here, it is difficult to provide the complete structural environments of these metal-carboxylates. However, based on the infrared spectral shifts, it may be concluded that these carboxylates experience interactions with Ni(II) in the following order: oxalate (strongest) > malate=citrate > malonate > lactate (weakest).
- 3) Concentration of different carboxylate species (free, metal-complexed) may not be obtained from the information presented here. Results presented here are for the dominant species present in solution, and metal-ligand complexes other than those presented here may occur, but at low concentration.
- 4) Stability constants reported in the literature are used to predict the a priori concentrations of different Ni(II)-carboxylate species. Although some of the spectral data is not in agreement with the stability constants of mono and polycarboxylates discussed in (1) and for malonate, accurate stability constants could not be derived from the spectra. This is because the concentrations of the weakly interacting species could not be determined.
- 5) Ni(II) complexation with soil fulvic acid is consistent with inner-sphere coordination by one or more carboxylate groups, but the XAFS spectra are noisy and outer-sphere modes of coordination cannot be ruled out.

Molecular interactions identified for Ni(II) may also be found with other metal ions in natural aquatic environments, and their interactions with carboxylate-containing ligands are vital to a number of natural processes. Although this study focuses on interactions between Ni(II) and a small number of structurally related carboxylic acids, the results can be applied to understand the interactions between Ni(II) and more complex macromolecules that contain the carboxylate functional groups in their structure (e.g., humic substances, proteins), and mineral-water interfacial reactions involving metal-carboxylates. The results of this study also highlight many of the inherent limitations in the current techniques used for characterizing aqueous metal-ligand complexes, particularly those that are not strongly complexed. This observation points to the need for further development of new techniques and methods that can provide unequivocal information on the structure and bonding of weaker metal-ligand complexes in aqueous systems. For example, recent developments in the application of soft X-ray absorption spectroscopy to aqueous samples hold special promise for characterizing these interactions.

Acknowledgments—This work was supported by the National Science Foundation (Chemical Sciences), the U.S. Department of Energy (Geosciences), and the Center for Environmental Bioinorganic Chemistry (CEBIC; supported by grants from NSF and DOE). We also thank the staff of SSRL for their assistance; Sam Webb (SSRL) for guidance with XAFS data analysis; F.M.M. Morel, J. Majzlan, and M. Hay (Princeton University) for valuable comments and discussion. We also acknowledge the thoughtful comments provided by three anonymous reviewers.

Associate editor: G. Sposito

REFERENCES

- Alcacio T. E., Hesterberg D., Chou J. W., Martin J. D., Beauchemin S., and Sayers D. E. (2001) Molecular scale characteristics of Cu(II) bonding in goethite-humate complexes. *Geochim. Cosmochim. Acta* **65**, 1355–1366.
- Ankudinov A. L., Ravel B., Rehr J. J., and Conradson S. D. (1998) Real space multiple scattering calculation and interpretation of X-ray absorption near edge structure. *Phys. Rev. B* **58**, 7565.
- Axe K. and Persson P. (2001) Time-dependent surface speciation of oxalate at the water-boehmite (γ -AlOOH) interface: Implications for dissolution. *Geochim. Cosmochim. Acta* **65**, 4481–4492.
- Baker E. N., Baker H. M., Anderson B. F., and Reeves R. D. (1983) Chelation of nickel(II) by citrate. The crystal structure of nickel-citrate complex $K_2[Ni(C_6H_5O_7)(H_2O)_2] \cdot 4H_2O$. *Inorg. Chim. Acta* **78**, 281–285.
- Bell C. F. (1977) *Principles and Applications of Metal Chelation*. Clarendon Press.
- Bickley R. L., Edwards H. G. M., and Rose S. J. (1990) A Raman spectroscopic study of nickel(II) acetate, $Ni(CH_3COO)_2$ and its aqueous and methanolic solutions. *J. Mol. Struct.* **238**, 15–26.
- Blesa M. A., Weisz A. D., Morando P. J., Salfity J. A., Magaz G. E., and Regazzoni A. E. (2000) The interaction of metal oxide surfaces with complexing agents dissolved in water. *Coord. Chem. Rev.* **196**, 31–63.
- Boily J. F., Nilsson N., Persson P., and Sjöberg S. (2000) Benzenecarboxylate surface complexation at the goethite (α -FeOOH)/water interface: I. A mechanistic description of pyromellitate surface complexes from the combined evidence of infrared spectroscopy, potentiometry, adsorption data, and surface complexation modeling. *Langmuir* **16**, 5719–5729.
- Buerge I. J. and Hug S. J. (1998) Influence of organic ligands on chromium(VI) reduction by iron(II). *Environ. Sci. Technol.* **32**, 2092–2099.
- Cabaniss S. E., Leenheer J. A., and McVey I. F. (1998) Aqueous infrared carboxylate absorbances: Aliphatic di-acids. *Spectrochim. Acta, Part A* **54**, 449–458.
- Cabaniss S. E. and McVey I. F. (1995) Aqueous infrared carboxylate absorbances: Aliphatic monocarboxylates. *Spectrochim. Acta, Part A* **51**, 2385–2395.
- Chen D. H. and Hsieh C. H. (2002) Synthesis of nickel nanoparticles in aqueous cationic surfactant solutions. *J. Mater. Chem.* **12**, 2412–2415.
- Colpas G. J., Maroney M. J., Bagyinka C., Kumar M., Willis W. S., Suib S. L., Baidya N., and Mascharak P. K. (1991) X-ray spectroscopic studies of nickel complexes with application to the structure of nickel sites in hydrogenases. *Inorg. Chem.* **30**, 920.
- Davies C. W. (1962) *Ion Association*. Butterworth.
- Deacon G. B. and Phillips R. J. (1980) Relationship between the carbon-oxygen stretching frequencies of carboxylate complexes and the type of carboxylate coordination. *Coord. Chem. Rev.* **33**, 227–250.
- Dobson K. D. and McQuillan A. J. (1999) In situ infrared spectroscopic analysis of the adsorption of aliphatic carboxylic acids to TiO_2 , ZrO_2 , Al_2O_3 , and Ta_2O_5 from aqueous solutions. *Spectrochim. Acta, Part A* **55**, 1395–1405.
- Downie T. C., Harrison W., Raper E. S., and Hepworth M. A. (1971) A three-dimensional study of the crystal structure of nickel acetate tetrahydrate. *Acta Cryst. B* **27**, 706–712.
- Edwards D. A. and Hayward R. N. (1968) Transition metal acetates. *Can. J. Chem.* **46**, 3443–3446.
- Ferry J. L. and Glaze W. H. (1998) Photocatalytic reduction of nitro organics over illuminated titanium dioxide: Role of the TiO_2 surface. *Langmuir* **14**, 3551–3555.
- Feth M. P., Klein A. and Bertagnolli H. (2003) Investigation of the ligand exchange behavior of square planar nickel(II) complexes by X-ray absorption spectroscopy and X-ray diffraction. *Eur. J. Inorg. Chem.* 839–852.
- Galoisy L. and Calas G. (1993) XANES and crystal-field spectroscopy of 5-coordinated nickel(II) in potassium-nickel phosphate. *Mater. Res. Bull.* **28**, 221–228.
- Gawel J. E., Ahner B. A., Friedland A. J., and Morel F. M. M. (1996) Role of heavy metals in forest decline indicated by phytochelatin measurements. *Nature* **381**, 64–65.
- George G. N., Pickering I. J. (1995) EXAFSPAK. Stanford Synchrotron Radiation Laboratory.
- Hind A. R., Bhargava S. K., Van Bronswijk W., Grocott S. C., and Eyer S. L. (1998) On the aqueous vibrational spectra of alkali metal oxalates. *Appl. Spectrosc.* **52**, 683–691.
- Hudson R. J. M. (1998) Which aqueous species control the rates of trace metal uptake by aquatic biota?. Observations and predictions of non-equilibrium effects. *Sci. Tot. Environ.* **219**, 95–115.
- Huheey J. E., Keiter E. A., Keiter R. L. (1993) *Inorganic Chemistry: Principles of Structure and Reactivity*. Harper Collins.
- Karlin K. D. (1993) Metalloenzymes, structural motifs, and inorganic models. *Science* **261**, 701–708.
- Koningsberger D. C. and Prins R. (1988) *X-ray absorption: Principles, applications, techniques of EXAFS, SEXAFS and XANES*. Wiley-Interscience.
- Kosugi N., Yokoyama T., and Kuroda H. (1986) Polarization dependence of XANES of square-planar $Ni(CN)_4^{2-}$ ion: A comparison with octahedral $Fe(CN)_6^{4-}$ and $Fe(CN)_6^{3-}$ ions. *Chem. Phys.* **104**, 449–453.
- Kubicki J. D., Blake G. A., and Apitz S. E. (1996) Molecular orbital models of aqueous aluminum-acetate complexes. *Geochim. Cosmochim. Acta* **60**, 4897–4911.
- Loring J. S., Karlsson M., Fawcett W. R., and Casey W. H. (2001a) Infrared spectra of phthalic acid, the hydrogen phthalate ion, and the phthalate ion in aqueous solution. *Spectrochim. Acta, Part A* **57**, 1635–1642.
- Loring J. S., Karlsson M., Fawcett W. R., and Casey W. H. (2001b) Speciation and complexation in aqueous Al(III)-quinolate solutions: A spectroscopic study. *Polyhedron* **20**, 1983–1994.
- Martell A. E. and Hancock R. D. (1996) *Metal Complexes in Aqueous Solutions*. Plenum Press.
- Martell A. E., Smith R. M. and Motekaitis R. J. (1997) Critically selected stability constants of metal complexes database. U.S. Department of Commerce, National Institute of Standards and Technology.
- Mehrotra R. C., Bohra R. (1983) *Metal Carboxylates*. Academic Press.
- Nachtegaal M. and Sparks D. L. (2003) Nickel sequestration in a kaolinite-humic acid complex. *Environ. Sci. Technol.* **37**, 529–534.
- Newville M. (2001) IFEFFIT: Interactive XAFS analysis and FEFF fitting. *J. Synchrotron Rad.* **8**, 322–324.
- Newville M., Livins P., Yacoby Y., Stern E. A., and Rehr J. J. (1993) Near-edge X-ray-absorption fine structure of Pb: A comparison of theory and experiment. *Phys. Rev.* **B47**, 14126–14131.
- Neys P. E. F., Vankelecom I. F. J., L'abbe M., Parton R. F., Cenlemans E., Dehaen W., L'abbe G., and Jacobs P. A. (1998) Manganese- and iron-porphyrins embedded in a polydimethylsiloxane membrane: A selective oxidation catalyst. *J. Mol. Catal. A* **134**, 209–214.
- Nicolai B., Kearley G. J., Johnson M. R., Fillaux F., and Suard E. (1998) Crystal structure and low-temperature methyl-group dynamics of cobalt and nickel acetates. *J. Chem. Phys.* **109**, 9062–9074.
- O'Day P. A., Rehr J. J., Zabinsky S. I., and Brown G. E. (1994) Extended X-ray absorption fine structure (EXAFS) analysis of disorder and multiple scattering in complex crystalline solids. *J. Am. Chem. Soc.* **116**, 2938–2949.
- Papelis C., Hayes K. F. and Leckie J. O. (1988) HYDRAQL: A program for the computation of chemical equilibrium composition of aqueous batch systems including surface-complexation modeling of ion adsorption at the oxide/solution interface. Stanford University.
- Penn R. L., Stone A. T., and Veblen D. R. (2001) Defects and disorder: Probing the surface chemistry of heterogenite (CoOOH) by dissolution using hydroquinone and iminodiacetic acid. *J. Phys. Chem. B* **105**, 4690–4697.
- Persson P., Karlsson M., and Öhman L. A. (1998) Coordination of acetate to Al(III) in aqueous solution and at the water-aluminum

- hydroxide interface: A potentiometric and attenuated total reflectance FTIR study. *Geochim. Cosmochim. Acta* **62**, 3657–3668.
- Pike P. R., Sworan P. A., and Cabaniss S. E. (1993) Quantitative aqueous attenuated total reflectance Fourier transform infrared spectroscopy. Part II. Integrated molar absorptivities of alkyl carboxylates. *Anal. Chim. Acta* **280**, 253–261.
- Quilès F., Burneau A., and Gross N. (1999) Vibrational spectroscopic study of the complexation of mercury(II) by substituted acetates in aqueous solutions. *Appl. Spectrosc.* **53**, 1061–1070.
- Ravel B (2002) ATOMS: crystallography for the X-ray absorption spectroscopist. *J Synchrotron Rad* **8**, 314–316.
- Rudolph W., Brooker M. H., and Tremaine P. R. (1997) Raman spectroscopic investigation of aqueous FeSO₄ in neutral and acidic solutions from 25°C to 303°C: Inner- and outer-sphere complexes. *J. Sol. Chem.* **26**, 757–777.
- Rudolph W. W., Brooker M. H., and Tremaine P. R. (1999) Raman spectroscopy of aqueous ZnSO₄ solutions under hydrothermal conditions: Solubility, hydrolysis, and sulfate ion pairing. *J. Sol. Chem.* **28**, 621–630.
- Ruiz-Pérez C., Hernández-Molina M., Sanchiz J., López T., Lloret F., and Julve M. (2000) Synthesis, crystal structure and magnetic properties of the three-dimensional compound [Na₂Ni(mal)₂(H₂O)₆]_n (H₂mal = malonic acid). *Inorg. Chim. Acta* **298**, 245–250.
- Sandstrom D. R. (1979) Ni²⁺ coordination in aqueous NiCl₂ solutions: Study of the extended X-ray absorption fine structure. *J. Chem. Phys.* **71**, 2381–2386.
- Scheidegger A. M., Lamble G. L., and Sparks D. L. (1996) Investigation of Ni sorption on pyrophyllite: An XAFS study. *Environ. Sci. Technol.* **30**, 548–554.
- Schmelz M. J., Nakagawa I., Mizushima S.-I., and Quagliano J. V. (1959) Infrared absorption spectra of inorganic coordination complexes. XVIII. Infrared studies of malonato metal complexes. *J. Am. Chem. Soc.* **81**, 287–290.
- Stumm W. and Morgan J. J. (1996) *Aquatic Chemistry: Chemical Equilibria and Rates in Natural Waters*. Wiley and Sons.
- Thurman E. M. (1985) *Organic Geochemistry of Natural Waters*. Martinus Nijhoff Publishers.
- Trivedi P., Axe L., and Tyson T. A. (2001) XAS studies of Ni and Zn sorbed to hydrous manganese oxide. *Environ. Sci. Technol.* **35**, 4515–4521.
- Webb S. (2003) SixPACK: Sam's interface for XAS package, Stanford Synchrotron Radiation Laboratory.
- Xia K., Bleam W., and Helmke P. A. (1997) Studies of the nature of binding sites of first row transition elements bound to aquatic and soil humic substances using X-ray absorption spectroscopy. *Geochim. Cosmochim. Acta* **61**, 2223–2235.